Supporting information for

Fiber-glass supported catalysis. Real-time, high-resolution visualization of active Palladium catalytic centers during the reduction of nitro compounds

Bowen Wang, Connor Bourgonje and Juan C. Scaiano*

Department of Chemistry and Biomolecular Sciences, University of Ottawa, Ottawa, Ontario, Canada K1N 6N5

CONTENT

Figure Content

1 Materials and methods

1.1 Materials

4-Nitro-1,8-naphthalic anhydride (95%), Butylamine (99.5%), Ethanolamine (98%), Glass Wool (Non-Treated, pkg of 50 g), Methanol (spectrophotometric grade > 99.8%), Hydrazine solution 35 wt.% in H_2O, Palladium(II) acetylacetonate (99%) were purchased from Sigma-Aldrich. Irgacure-2959 was a gift from BASF and I-907 from Ciba Specialty Chemicals. All solvents (HPLC grade) were dried using molecular sieves. The MilliQ water was obtained by purification of deionized water using a Thermo Scientific™ Barnstead™ GenPure™ water purification system (conductivity 18 MΩ cm^{-1}).

1.2 Instruments

The palladium (Pd) was grafted on the support by photo-doping using Irgacure 2959 (I-2959) as the photoinitiator under UVA irradiation (Luzchem LZC-4V photoreactor equipped with 8 UVA lamps).

NMR spectra were recorded at room temperature in a Bruker Avance 400 spectrometer. The palladium loading was analyzed by inductively coupled plasma atomic emission spectrometry (ICP-OES, Agilent 5110 VDV ICP-OES Spectrometer). The MS spectra were analyzed by electrospray ionization tandem mass spectrometry (ESI) (Agilent 6125B single quadrupole LC/MSD system). The optical characterization of the molecular probes in methanol was performed with a UV–visible spectrometer (Cary 100 or Cary 60, Agilent Technologies) and a fluorescence spectrometer (Photon Technology International).

The Total Internal Reflection Fluorescence Microscopy (TIRFM) experiments were carried out in a Nikon Eclipse Ti2 inverted microscope equipped with a Ti2 platform with motorized XYZ, motorized TIRF illumination, a Perfect System Focus to maintain focus through time, and an ANDOR iXon Ultra EM-CCD camera controlled by NIS-Elements software (Nikon, New York, NY, USA). The images were captured using an oil-immersion objective (SR HP Apo TIRF 100×H NA=1.49 WD=120μm) and irradiated with a 488 nm continuous wave (CW) laser light filtered through the excitation filter (483-494 nm). The light emitted was collected by the same objective and filtered with an emission filter (525-549 nm). An exposure time of 100 ms per frame was used. The data was analyzed by ImageJ and a home written Python program[1].

The confocal images were obtained using the Nikon A1 confocal microscope with 488 nm excitation continuous wave (CW) lasers. The high resolution 3-dimensional confocal image was generated from a stack of 2D images with a vertical spacing of 0.1 μm per image. All the images were processed by NIS-Elements software. FLIM image was acquired using the Becker and Hickl (B&H) FLIM module from Nikon. A 488 nm pulsed laser was employed in FLIM experiments. The lifetime of AN in FLIM images were analyzed by B&H SPCImage software. The B&H FLIM was equipped with B&H BDS-SM picosecond diode lasers that deliver picosecond light pulses (480.511 nm, 50MHz, BDS-488-SM-FBC). The fluorescence signal from NN to AN reaction were recorded by an SPC-150N TCSPC/FLIM module.

All microscope experiment reaction solutions were pumped into the flow cell using an NE-300 Just Infusion™ Syringe Pump.

1.3 Catalyst preparation

1.3.1 Glass wool pre-treatments

Firstly, 500 mg of as-purchased glass wool was washed with 1 M NaOH solution under sonication (15 min × 3) and rinsed with MilliQ water. After drying under argon, the glass wool was treated with piranha solution (3:1 concentrated sulfuric acid and 30% hydrogen peroxide solution) for 3 hours. Then the pre-treated glass wool was rinsed with MilliQ water and dried under argon.

1.3.2 Activation using (3-Aminopropyl) triethoxysilane (APTES)

The pre-treated glass wool was immersed in 1% APTES solution in toluene (99.5%) and refluxed overnight. After cooling down to room temperature, the APTES-treated glass wool was washed with toluene (5×), methanol (5×), and MilliQ water (5×) before drying under argon. The APTES-treated glass wool was then ground to small pieces and kept under argon.

1.3.3 Palladium decoration

The palladium was deposited on glass wool by a photo-doping method using I-2959 (**1**) as photoinitiator[2]. The ketyl radicals (**3**) were generated under UVA irradiation by Norrish Type I cleavage. The active radicals generated then reduce Pd^{2+} into Pd^{0}. The Pd^{0} aggregate to Pd cluster or Pd nanoparticles and attached on the surface of APTES-modified glass wool. Briefly, 500 mg of APTES-modified glass wool were immersed in 150 mL MeOH solution of 75mg $Pd(acac)_2$ and 113 mg of I-2959. The system was purged with argon for 15 min and left under UVA irradiation for 4 hours. The palladium modified glass wool (Pd-GW) was then washed with MeOH (3×) and MilliQ (3×) to remove unattached Pd particles and organic residue. The clean Pd@GW was dried and stored under argon for future use. The Pd loading Pd@GW was 2.0± 0.3% by ICP-OES.

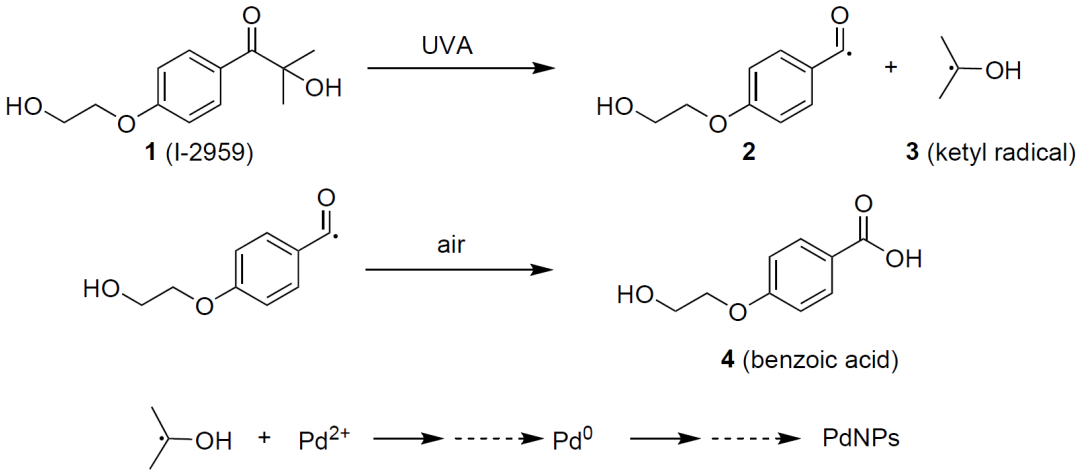

Scheme S1: Photolysis of I-2959 and its radical products in the synthesis of Pd nanoparticles. The benzoyl radical (2) form corresponding benzoic acid (3). This benzoic acid will become a surfactant on the surface of Pd nano particles. In early report, the benzoic acid will stabilize the metal nanoparticles.[3] In order to avoid the effects from the organic residuals in microscopy experiments, all the catalysts went through an annealing process before the microscope experiment.

1.4 Synthesis of Nitronaphthalimide

1.4.1 Synthesis of NN1

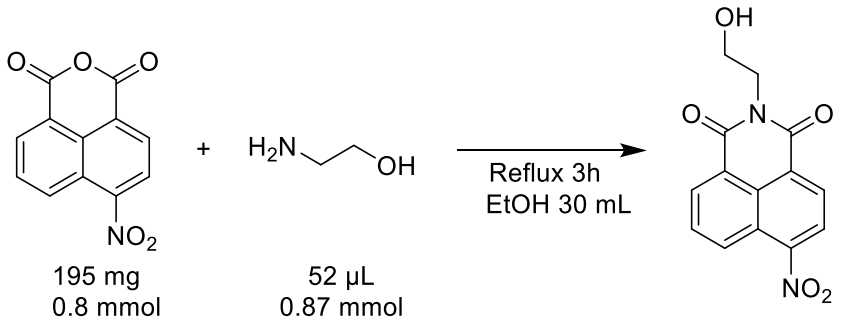

Scheme S2: Synthesis of NN1

4-nitro-1,8-naphthalic anhydride (195 mg, 0.8 mmol) and ethanolamine (52 µL 0.87 mmol) were dissolved in 30 mL ethanol and under refluxed for 3 hours. After cooling down to room temperature, the solvent was removed under reduced pressure. The product was purified by recrystallization, yielding NN1, light yellow needle-like crystals. The NMR, ESI, absorption, and fluorescence spectra were shown in SI section 5.

1.4.2 Synthesis of NN2

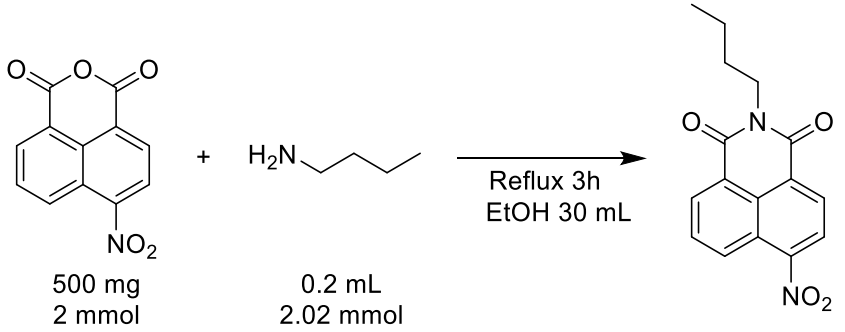

Scheme S3: Synthesis NN2

4-nitro-1,8-naphthalic anhydride (500 mg, 2 mmol) and butylamine (200 µL 2.02 mmol) were dissolved in 30 mL ethanol and under refluxed for 2 hours. After cooling down to room temperature, the solvent was removed under reduced pressure. The product was purified by a flash column. The NMR, ESI, absorption, and fluorescence spectra were shown in in SI section 5.

1.4.3 Synthesis of NN2-NHOH

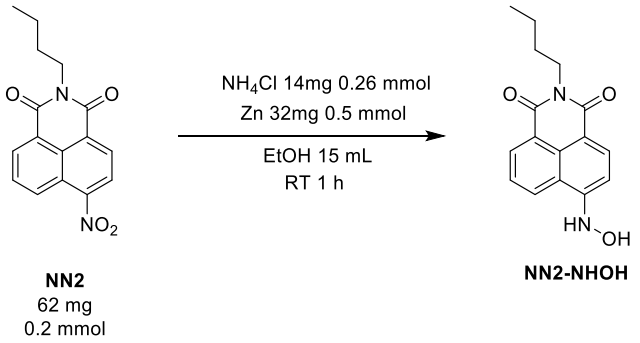

Scheme S4: Synthesis NN2-NHOH

NN2 (62 mg, 0.2 mmol) and ammonium chloride (14mg, 0.26mmol) was dissolved in 15 mL ethanol. After adding 32 mg of zinc particles, the system was stirred at room temperature for 1 hour. The zinc particles were removed by centrifuge and concentrated under reduced pressure. The product was analyzed by HPLC-MS.

2 Nitronaphthalimides reduction bench scale reaction

In order to investigate the nitronaphthalimides reduction reaction mechanism, we first examined NN1 and NN2 reduction on bench scale reaction under different conditions. The two dyes were produced to investigate the behavior of the dye in aqueous (NN1) and organic (NN2) environments.

2.1 NN2 reduction reaction using H_2 as reduce agent

NN2 was first reduced by hydrogen gas in present of Pd@GW. 3mL of 0.1 mM NN2 was dissolved in MeOH and 7 mg Pd@GW, Scheme S5. A continues hydrogen was purged in the system. The reaction was monitored by UV-vis.

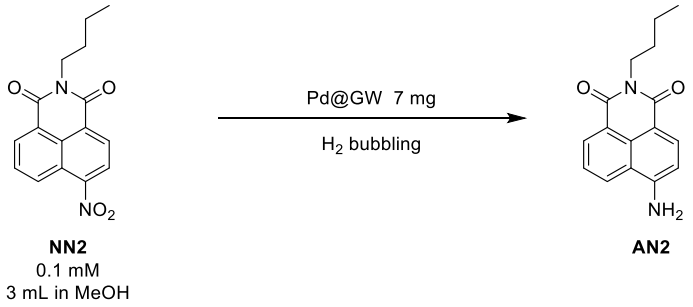

Scheme S5: Reduction of the fluorogenic probe NN2 by Pd@GW using H_2

The UV absorption of system was shown in Figure S1. From the Figure S1, the NN2 peak (black line) decreased and showed a new peak around 440 nm in 5 minutes. The result shows that the NN2 was reduced to AN2 in 5 minutes in the presence of hydrogen bubbling and Pd@GW. During the reaction, Pd@GW could be removed easily by tweezers (insert image) before the UV-Vis characterization. Compared with a long-time centrifuge post-process when using P25 based catalyst, the Pd@GW could provide an easy and fast separation process after reaction.

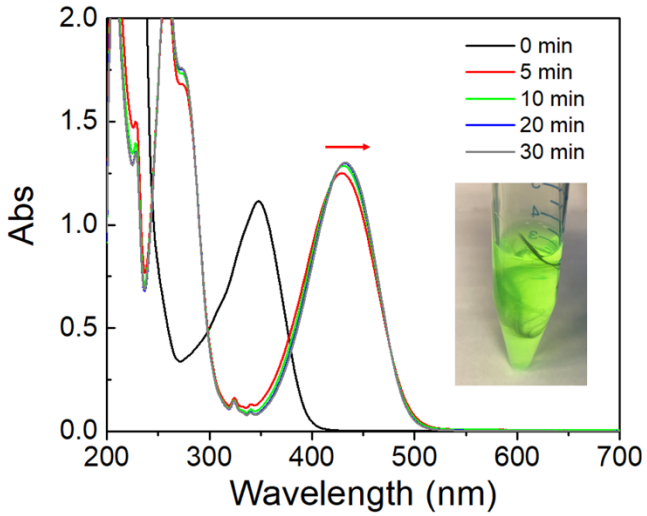

Figure S1: Reduction of the fluorogenic probe NN2 by Pd@GW. Reaction conditions: 3 mL of 0.1 mM NN2 MeOH solution was added 7 mg Pd@GW, the system was gently bubbled with H_2 flow. The UV absorption spectrum were recorded by Cary 60 spectrometer. Inset image: Pd@GW catalyst in the reaction media after reduction. The color of solution changed from colorless to light green. The fibre catalysts were easily removed from the dye solution with tweezers for UV-Vis measurements.

From Figure S1, we could find a small red shift of product absorption in the first 5 min. Based on direct reduction route of aromatic nitro compound [4] we believe a hydroxylamine (NN2-NHOH) intermediate was formed during the reaction using H_2. In order to prove our idea, NN2-NHOH was synthesized. The UV-vis of NN2-NH-OH were shown in Figure S2 (ESI in Figure S20). From the UV-vis of NN2-NHOH, the absorption is matched with the intermedia in the NN2 reduction reaction using H_2.

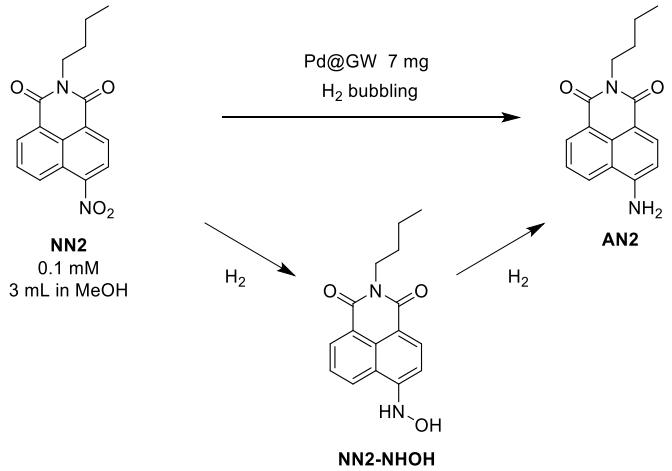

Scheme S6: Proposed reaction pathways for NN2 reduction reaction under H_2 bubbling.

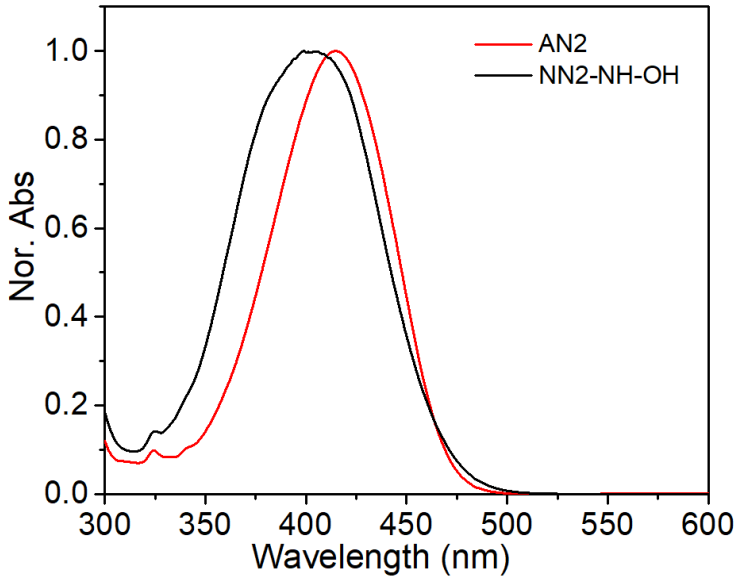

Figure S2: Normalized UV spectra of NN2-NHOH and AN2. The NN2-NH-OH and AN2 isolated products were purified by Preparative HPLC Systems. The UV absorption spectra were recorded by HPLC UV-vis detector, HPLC flow phase 99% CH_3CN and 1% water.

2.2 NN2 reduction reaction using N_2H_4 as reducing agent

Nitronaphthalimides reduction reaction also tested by using N_2H_4 as reducing agent. 7 mg of Pd@GW and 160 µL of 35% N_2H_4 were added to 3 mL of 0.1 mM of NN2 in methanol, the NN2 was fully reduced to AN2 in 15 min, Figure S3 (a). An intermediate with absorption at 550nm was observed in present of N_2H_4. Those intermediates all fully convert to the AN2 at end of the reaction. Two blank experiments were shown in Figure S3(b) and (c). The NN2 reduction reaction without catalyst was shown in Figure S3 (b). We could find that the NN2 solution is stable in present of Pd@GW for a long time. The reaction kinetics without Pd@GW were shown in Figure S3 (c). The reaction was not finished after 10 hours compared with 15 min in the presence of Pd@GW.

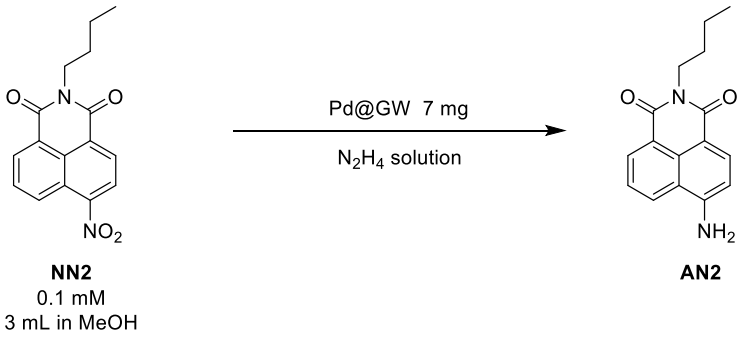

Scheme S7: Reduction of the fluorogenic probe NN2 by Pd@GW using N_2H_4

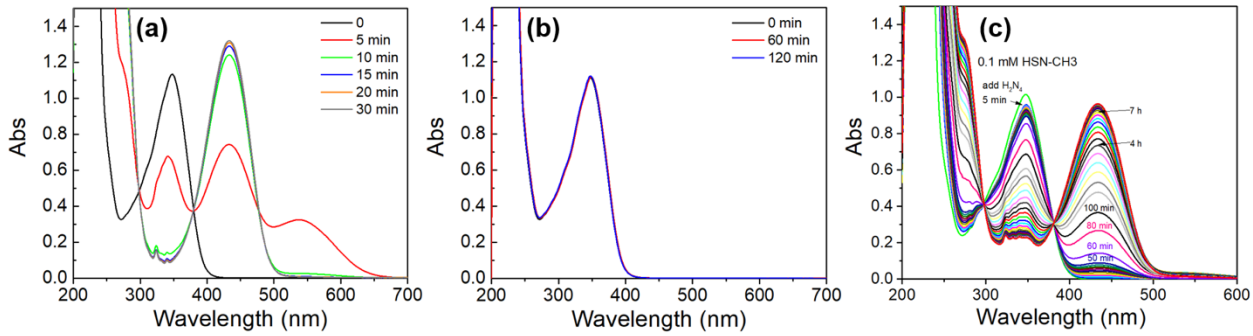

Figure S3: (a) 0.1 mM NN2 reduction reaction using 7 mg of Pd@GW and N_2H_4 (160 µL 35% N_2H_4) as reducing agent; (b) Control experiment: 0.1 mM NN2 solution with 7 mg Pd@GW; (c) 0.1 mM NN2 solution with 160 µL 35% N_2H_4.

From Figure S3 (a), we found the NN2 reduction reaction to have a different intermediate when using H_2 or N_2H_4. While the intermediate will convert to AN2 at end, those intermediates may affect the sensitive microscopy experiment. In order to decrease the influence from the reaction intermediate in single molecule reaction, a series of experiments were designed. The effect of pH was investigated by adding acetic acid or NaOH in NN2 reduction reaction solution. From Figure S4, we could find that acid additive will selectively obtain AN2 product without the formation of a long wavelength intermediate. From the nitro compounds reduction mechanism[4, 5], we believe that azo- and azoxy-aromatics products are the intermediates which could be achieved in present of under basic conditions. Similar reactions were applied in 25 µM system (same concentration for most microscopy experiment), as shown in Figure S5.

In conclusion, from Figure S4 and Figure S5, we find the acid additive could avoid both NN-NHOH and azo-/azoxy by-products, making it essential to our single molecule experiments.

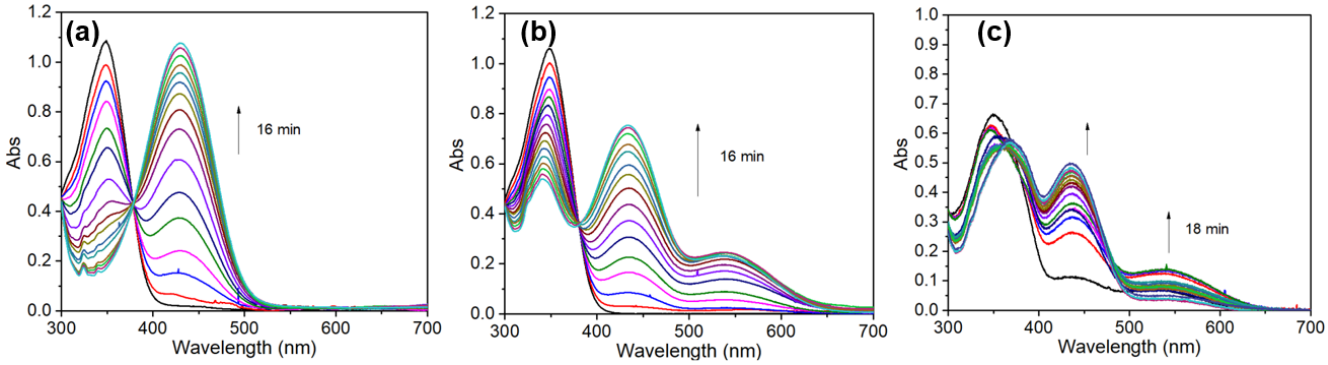

Figure S4: 0.1 mM NN2 reduction reaction using 7 mg of Pd@GW and N_2H_4 (160 µL 35% N_2H_4) as reducing agent in the presence 100 µL 3.3M acetic acid (a), 100 µL MilliQ H_2O (b), and 100 µL 3.3M NaOH (c).

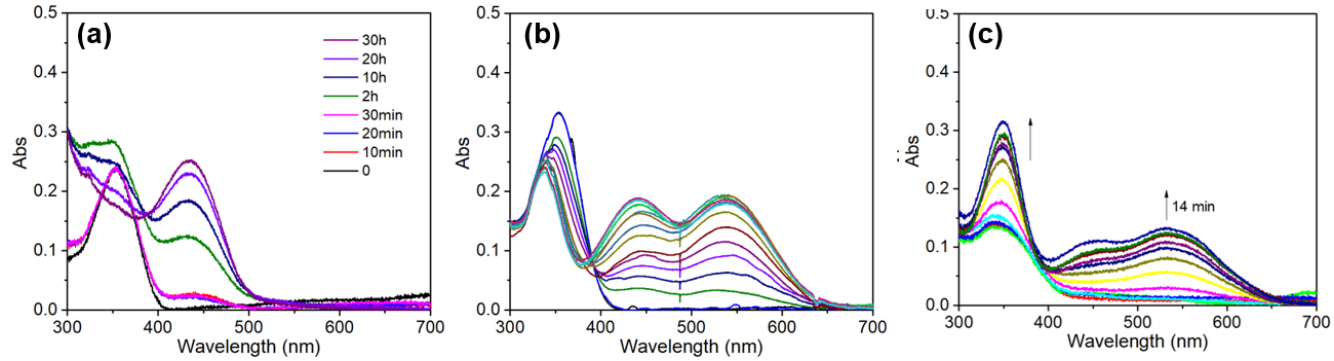

Figure S5: 0.5 mL of 0.01 mM NN2 reduction reaction using 7 mg of Pd@GW and N_2H_4 (160 µL 0.35% N_2H_4) as reducing agent in the presence of 1.5 mL 3.3M acetic acid (a), 1.5 mL MilliQ H_2O (b) and 1.5 mL 3.3M NaOH (c).

2.3 NN1 reduction reaction using N_2H_4 as reducing agent

Nitronaphthalimides reduction reaction also tested by using NN1 in aqueous solution using N_2H_4 as reducing agent. 7 mg of Pd@GW, 160 µL of 35% N_2H_4, and 100 µL 3.3 M acetic acid were added to 3 mL of 0.1 mM of NN1 in MilliQ water. The reaction kinetics are shown in Figure S6 (a). Like the NN2 reduction, there is not NHOH or azo- by-products under acidic conditions. Two blank experiments were shown in Figure S6 (b) and (c). The NN1 is stable in water without N_2H_4. The reduction reaction required almost 2 days to complete in the absence of the catalyst.

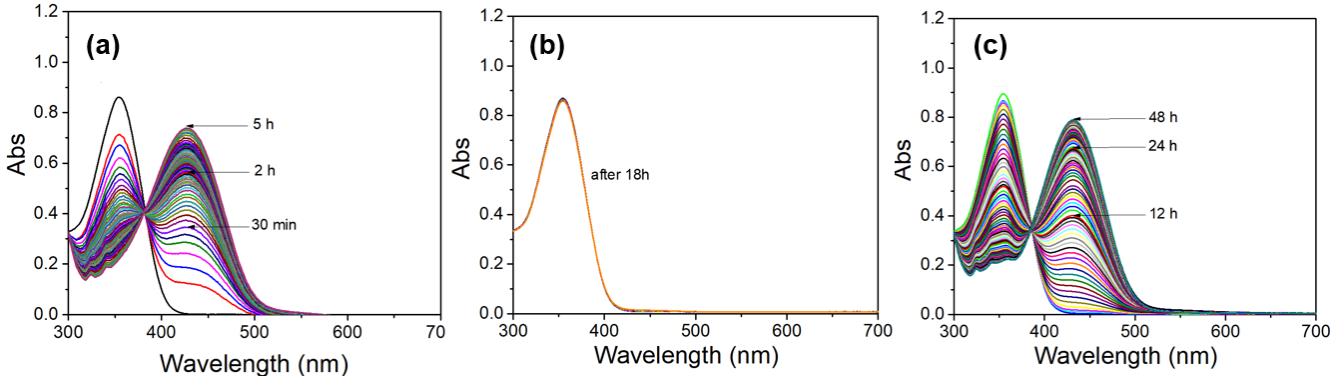

Figure S6: (a) 0.1 mM NN1 reduction reaction using 7 mg of Pd@GW, N_2H_4 (160 µL 35% N_2H_4), and 100 µL 3.3 M acetic acid; (b) 0.1 mM NN1 reduction reaction using 7 mg of Pd@GW and 100 µL 3.3M acetic acid without reduce agent.; (c) 0.1 mM NN1 reduction reaction using N_2H_4 (160 µL 35% N_2H_4) and 100 µL 3.3 M acetic acid without catalyst.

Similar reactions were applied in 1 µM NN1 system (same concentration for most microscopy experiment), as shown in Figure S7.

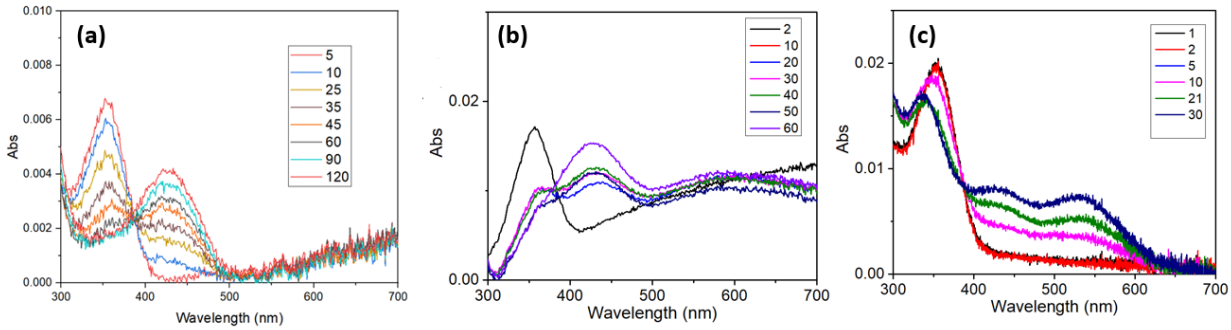

Figure S7: 1 µM NN1 reduction reaction using 7 mg of Pd@GW and N_2H_4 (160 µL 0.35% N_2H_4) as reducing agent in the presence of 100 µL 0.033 M acetic acid (a), 100 µL MilliQ H_2O (b) and 100 µL 0.033 M NaOH (c). The absorption above 500 nm was from the scattering from Pd@GW catalyst

3 Single molecule, Confocal and FLIM reaction conditions

3.1 Catalyst loaded coverslip preparation

The Pd@GW catalysts were deposited on a glass coverslip and placed in an oven for annealing process at 500 ℃ to burn off any organic residue before microscope experiments. The loaded coverslip was cooled down to room temperature and placed in a flow cell (Live Cell Instrument, Chamlide model CF-S25-B-C) for the experiment.

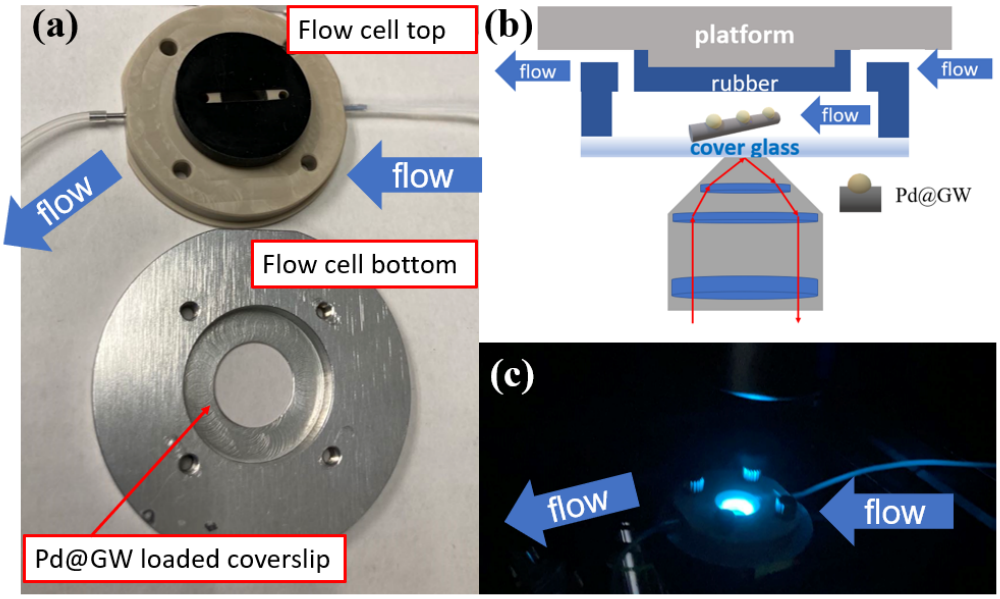

Figure S8: (a) Picture of flow cell, a Pd@GW loaded coverslip was placed in the flow cell bottom. (b) Scheme of flow cell mounted on the top of objective and laser light path. (c) Mounted flow cell in the microscope, the blue light in the middle of flow cell from the 488 nm laser.

3.2 Single molecule experiments

1 mL of 1μM NN1 water solution, 160 μL of N_2H_4 solution (35%, ×100 dilution in water) and 100 μL of acetic acid (0.033M in water) were premixed and injected into the flow cell immediately. The reaction solution was introduced into the flow cell using a syringe pump with 0.5mL/h speed.

3.3 Confocal experiment with 0.1mM NN1 (Figure 2, Figure 3)

Following the single molecule experiment, 1 mL of 0.1mM NN1 water solution, 160 μL of N_2H_4 solution (35%, in water) and 100 μL of acetic acid (3.3M in water) were premixed and injected into the flow cell immediately. The reaction solution was introduced into the flow cell using a syringe pump with 0.5mL/h speed. The NIKON system was switched to Confocal control module for imaging. Image was the result from 4 averages with dwell time of 6.2 μs. The fiber ROI image size is 1024×512 pixels. The pixels size is 70 nm.

3.4 Confocal experiment with different concentration solution (Figure 4)

Different concentrations of NN1 water solution, 160 μL of N_2H_4 solution (35%, in water) and 100 μL of acetic acid (3.3 M in water) were premixed and injected into the flow cell immediately. The reaction solution was introduced into the flow cell using a syringe pump with 0.5 mL/h speed. The flow cell was pre-rinsed with 0.3 mL of the respective solution before recording each trial. A 50 s 'Time measurement' was applied during the flow reaction. Image was the result from a dwell time of 0.49 μs. The fiber ROI image size is 1024×256 pixels. The pixels size is 120 nm.

3.5 Confocal experiment with 0.1mM NN1 (Figure 5)

Following the single molecule experiment, 1 mL of 0.1 mM NN1 water solution, 160 μL of N_2H_4 solution (35%, in water) and 100 μL of acetic acid (3.3 M in water) were premixed and injected into the flow cell immediately. The reaction solution was introduced into the flow cell using a syringe pump with 0.5mL/h speed. The NIKON system was switched to Confocal control module for imaging. Image was the result from 8 averages with dwell time of 2.4 μs. The fiber ROI image size is 2048×2048 pixels. The pixels size is 40nm.

3.6 Confocal experiment with 0.1mM NN1 (Figure 7)

Following the single molecule experiment, 1 mL of 0.1 mM NN1 water solution, 160 μL of N_2H_4 solution (35%, in water) and 100 μL of acetic acid (3.3 M in water) were premixed and injected into the flow cell immediately. The reaction solution was introduced into the flow cell using a syringe pump with 0.5mL/h speed. The NIKON system was switched to Confocal control module for imaging. Image was the result from 8 averages with dwell time of 2.4 μs. The fiber ROI image size is 1024×1024 pixels. The pixels size is 100nm.

3.7 FLIM experiment

Without moving the sample, the reaction of NN1 to AN1 was examined by B&H FLIM control module in the NIKON system. The instrument was equipped with B&H BDS-SM picosecond diode lasers deliver picosecond light pulses (480.511 nm, 50MHz, BDS-488-SM-FBC). The laser beam is reflected down into microscope beam path by a dichroic mirror. A lens (oil-immersion objective, SR HP Apo TIRF 100×H NA=1.49 WD=120 μm) focuses the laser into sample plane. The fluorescence signal is collected back by the dichroic mirror and passes through a 488 longpass filter to an ID-100-50 SPAD detector. The FLIM data are recorded by SPC-150N TCSPC/FLIM module. The FLIM image was the result from 2 averages with dwell time of 28.8 μs. The fiber ROI image size is 1024×1024 pixels. The pixels size is 30 nm.

4 Catalyst SEM, TEM, and EDS analysis

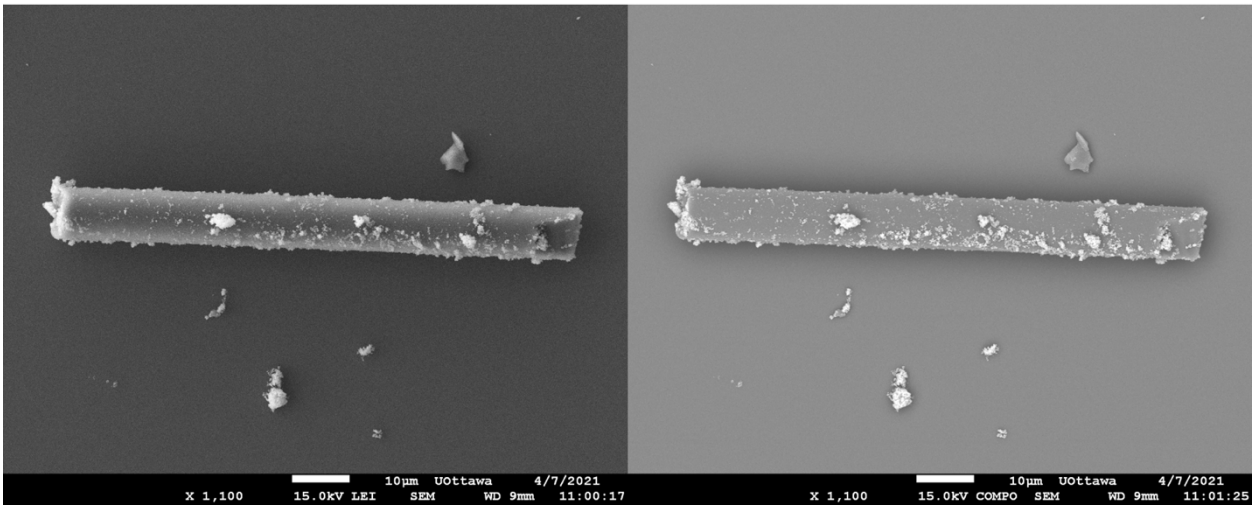

Figure S9: Representative SEM images of representative Pd@GW on a coverslip after the microscope experiment. Left: COMPO image. COMPO is a technique that shows heavier elements as brighter and lighter elements are darker, thus allowing for easy differentiation between metals and support.

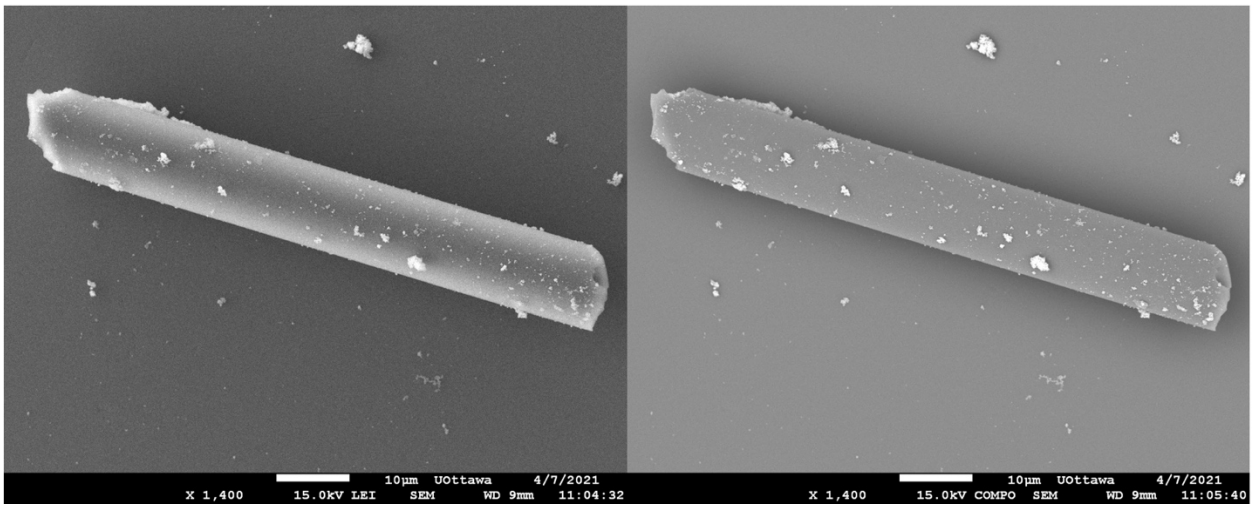

Figure S10: Representative SEM images of representative Pd@GW on coverslip after the microscope experiment. Left: COMPO image.

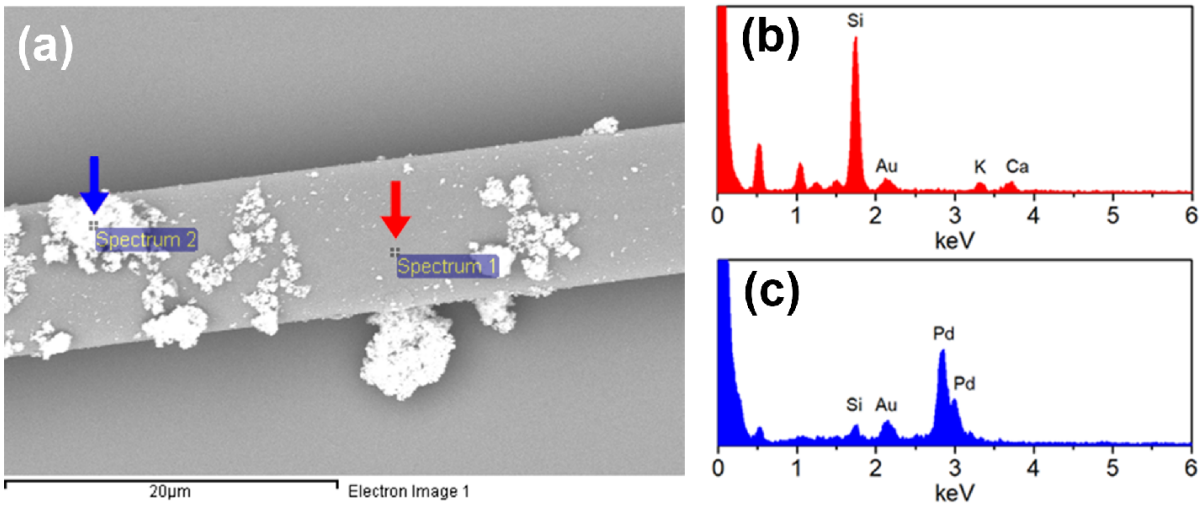

Figure S11: EDS analysis of Pd@GW on coverslip after microscope experiment. (a) SEM of Pd@GW, the lighter structure in the SEM (COMPO) image were Pd particles. (b) Representative EDS spectrum of surface without Pd decoration, the EDS scan area was shown by red arrow. (c) Representative EDS spectrum of surface with Pd decoration, the EDS scan area was shown by blue arrow. The EDS analysis of different areas on the same Pd@GW fiber SEM show the Pd structures were successfully decorated onto the GW surface.

It is important to understand the size of Pd nanoparticles of Pd@GW. However, the Pd@GW is too thick for TEM characterization. To observe Pd@GW in nano scale, the Pd@GW was ground and disperse in EtOH, the suspension of fragments of Pd@GW was dropped on the TEM grid. From the Figure S13, we could find that after the grinding, a small piece of Pd@GW broke off from the main catalyst chunk. The big Pd clusters were still difficult to analysis the size distribution, Figure S13(a) left-top. The size distribution was analysis by the individual Pd particles on the GW surface was shown in Figure S12.

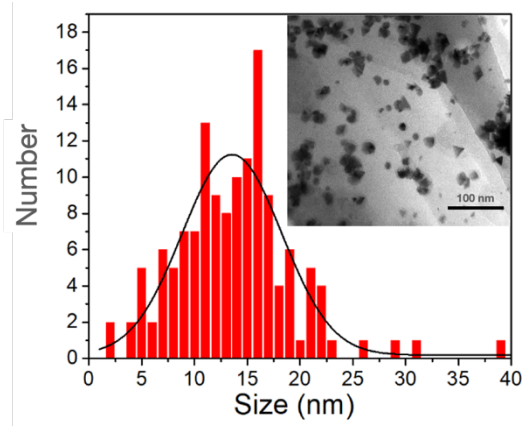

Figure S12 Particle size distribution for PdNP in Pd@GW. Inset: Representative TEM image of PdNPs on Pd@GW fragment. To observe nanometric features in Pd@GW by TEM, the Pd@GW was ground and dispersed in ethanol, the suspension of fragments of Pd@GW were drop-dried on the TEM grid. Note that in highly crowded regions it is not possible to measure individual particles. The region chosen has an intermediate particle density.

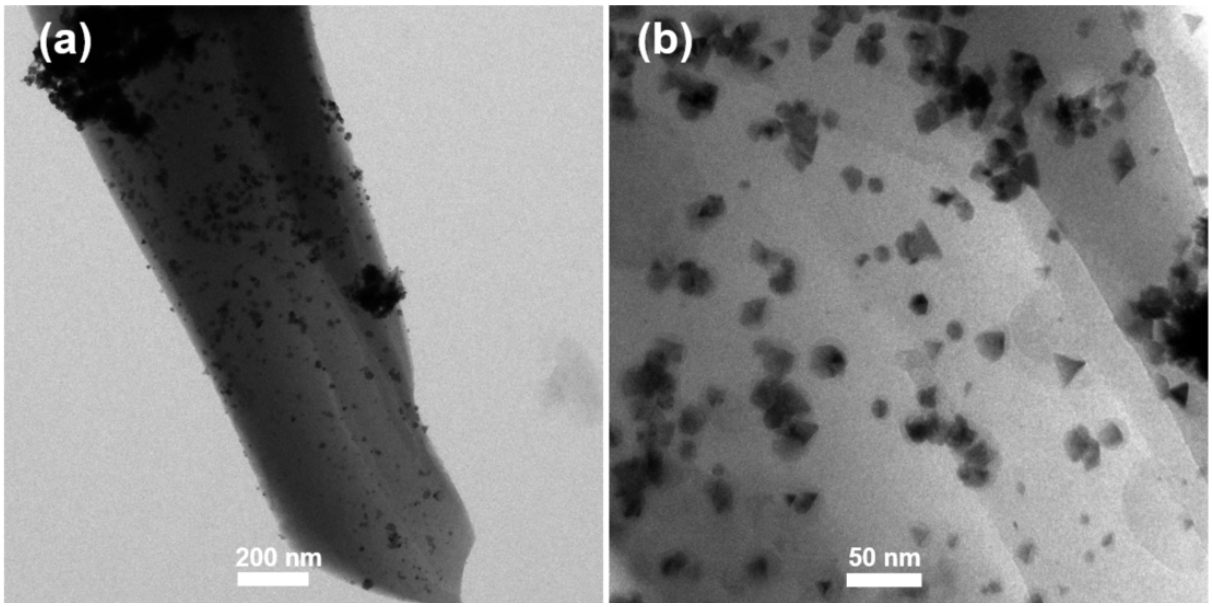

Figure S13: TEM images of representative fragments of Pd@GW.

~~6~~5 NMR, Mass Spectroscopy and Optical Spectroscopy

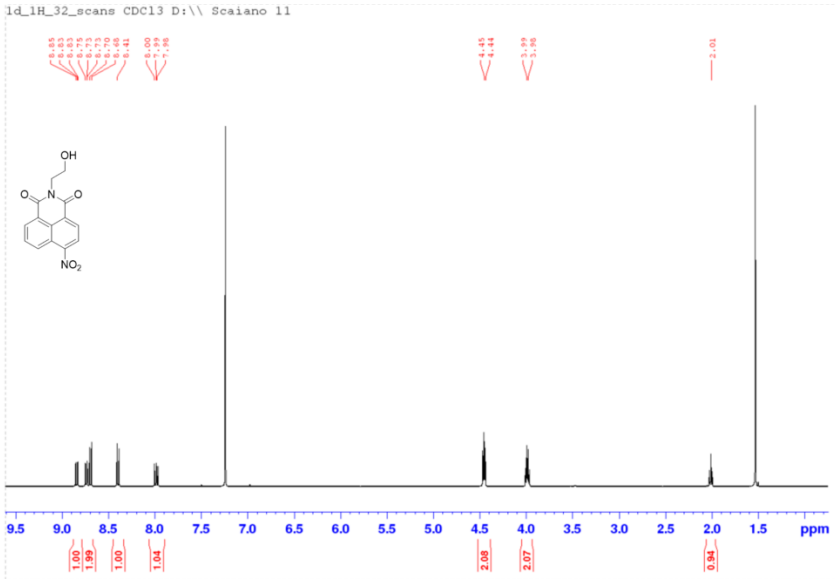

Figure S14: H-NMR of NN1 in $CDCl_3$

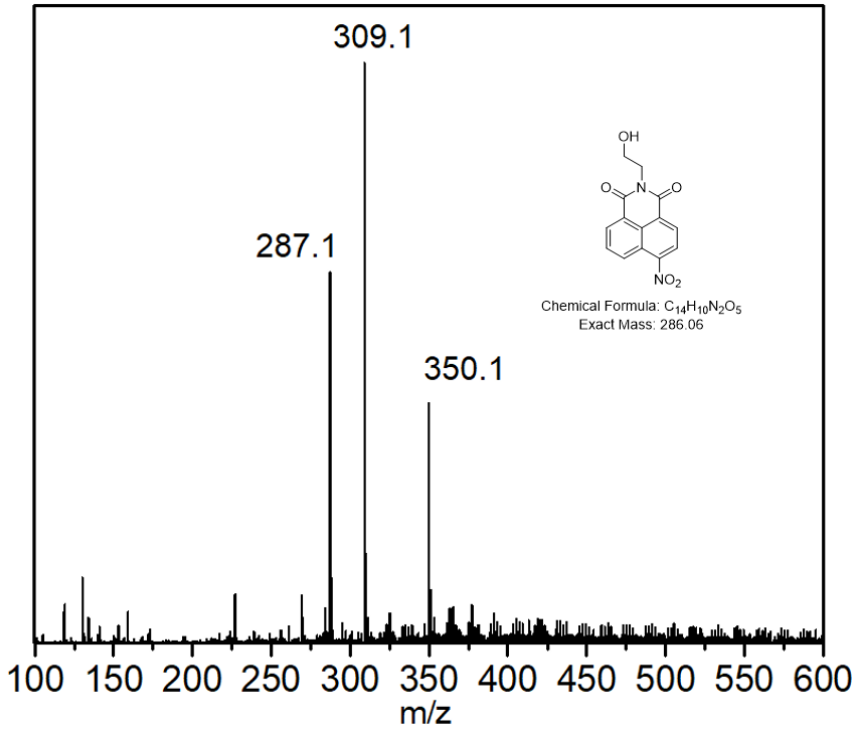

Figure S15: ESI of NN1, positive ESI source. $[NN1 + H]^+$: 287.1; $[NN1 + Na]^+$: 309.1; $[NN1 + CH_3CN + Na]^+$: 350.1

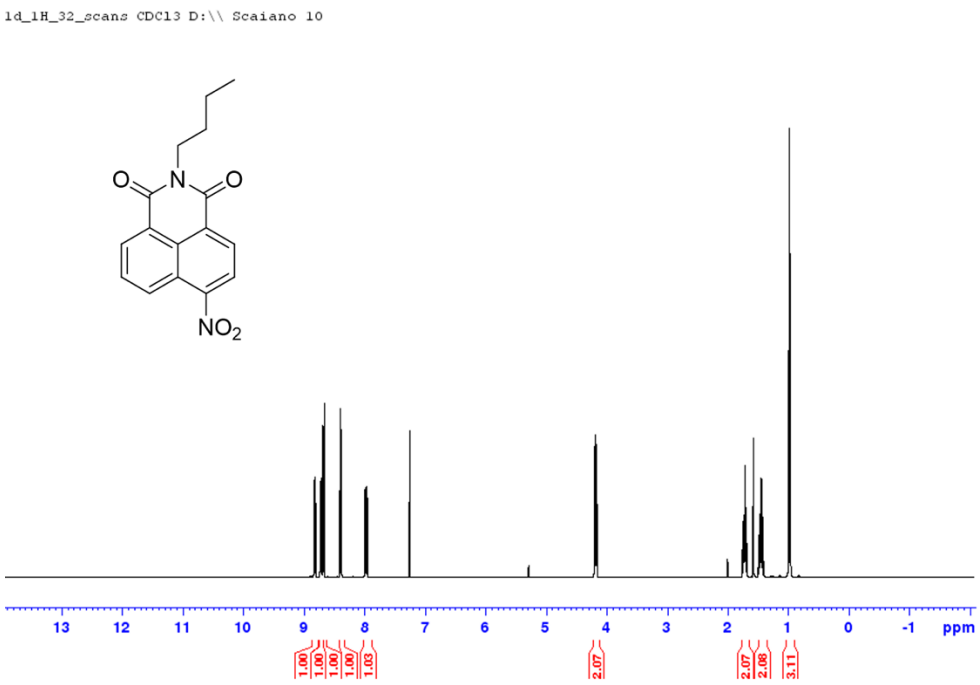

Figure S16: H-NMR of NN2 in $CDCl_3$

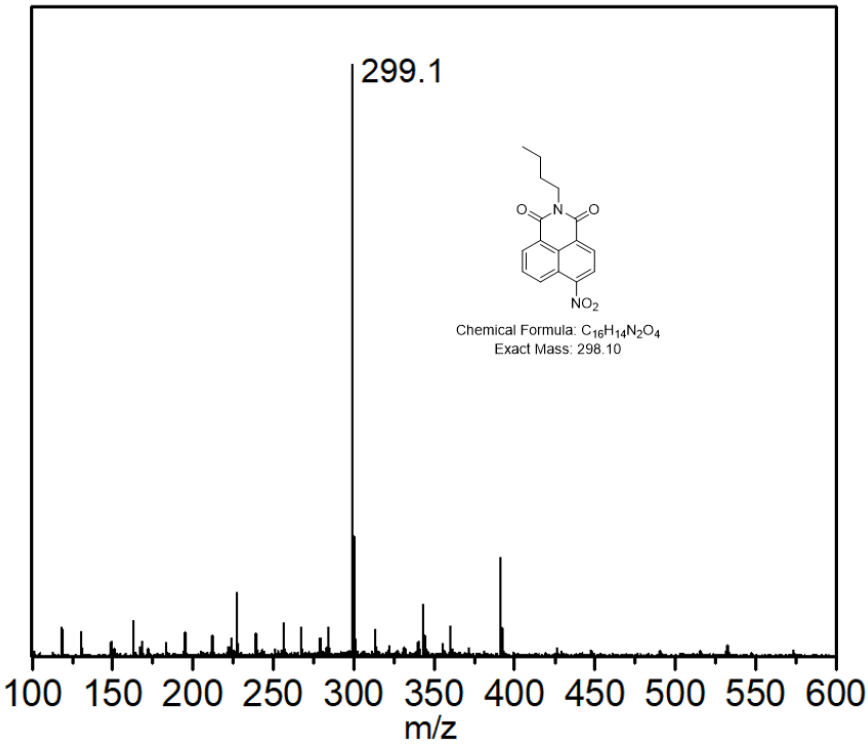

Figure S17: ESI of NN2, positive ESI source $[NN2 + H]^+$: 299.1.

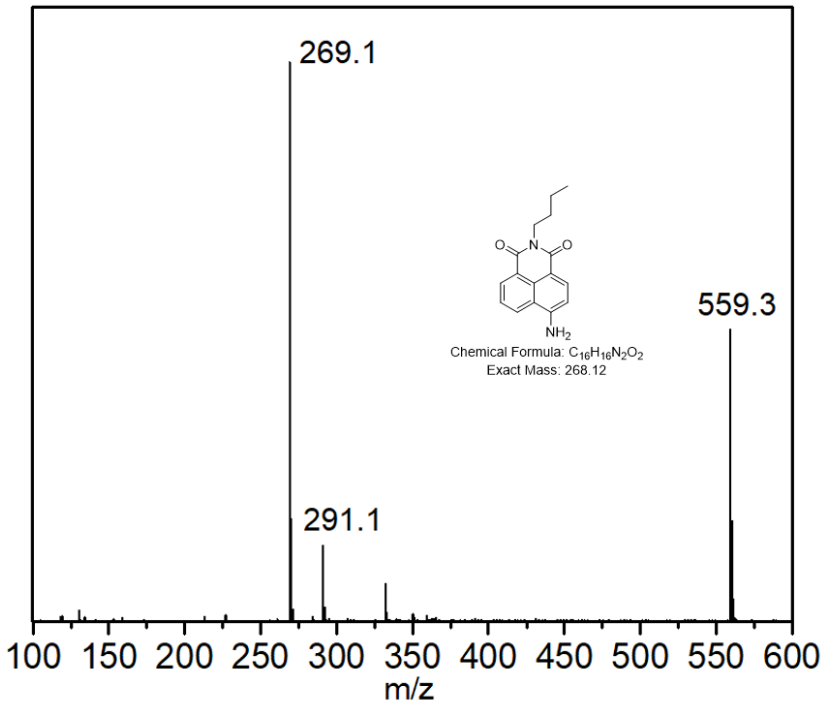

Figure S18: ESI of AN2, positive ESI source. $[AN2 + H]^+$: 269.1; $[AN2 + Na]^+$: 291.1; $[AN2 + AN2 + Na]^+$: 559.2

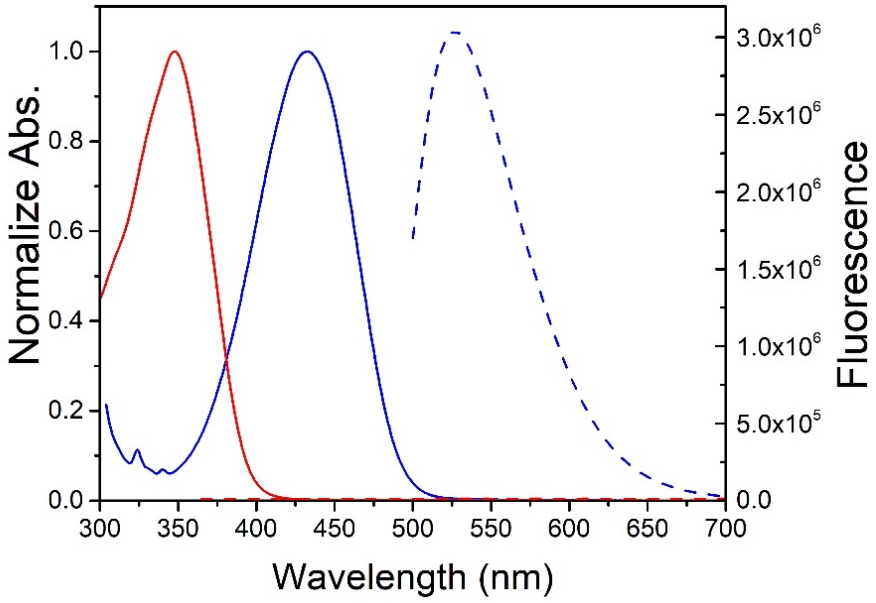

Figure S19: Normalized absorption (solid line) and fluorescence (dash line) spectra of NN2 (100 µM in water, red) and AN2 (100 µM in MeOH, blue). Excitation laser: λ_{ex}=350 nm for NN2, and λ_{ex}=488 nm for AN2. Note that fluorescence is not normalized and the difference in amplitude reflects the contrast of the dye emission intensity at equal concentration.

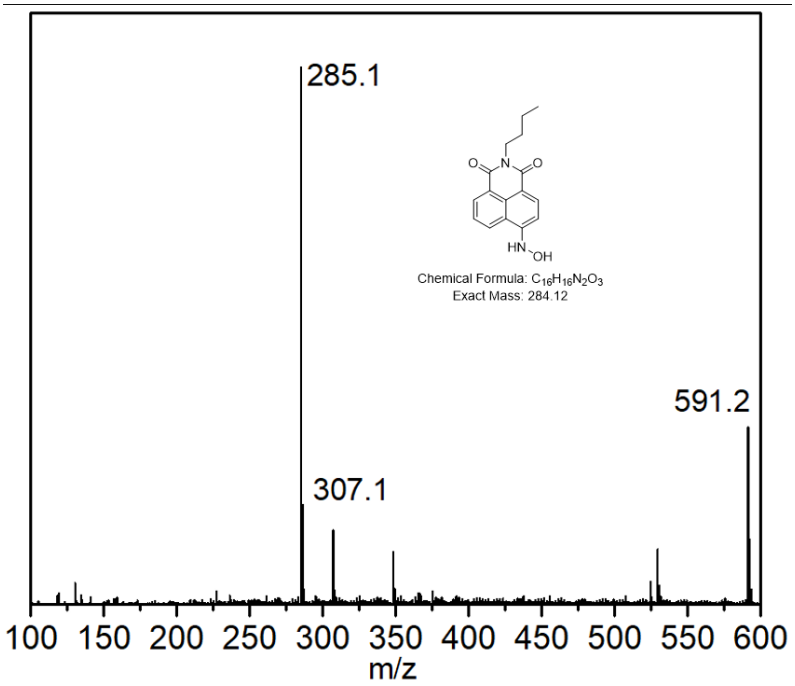

Figure S20: ESI of NN2-NHOH. $[NN2\text{-}NHOH + H]^+$: 285.1; $[NN2\text{-}NHOH + Na]^+$: 307.1; $[NN2\text{-}NHOH + NN2\text{-}NHOH + Na]^+$: 591.2

~~7~~6 Confocal Microscopy

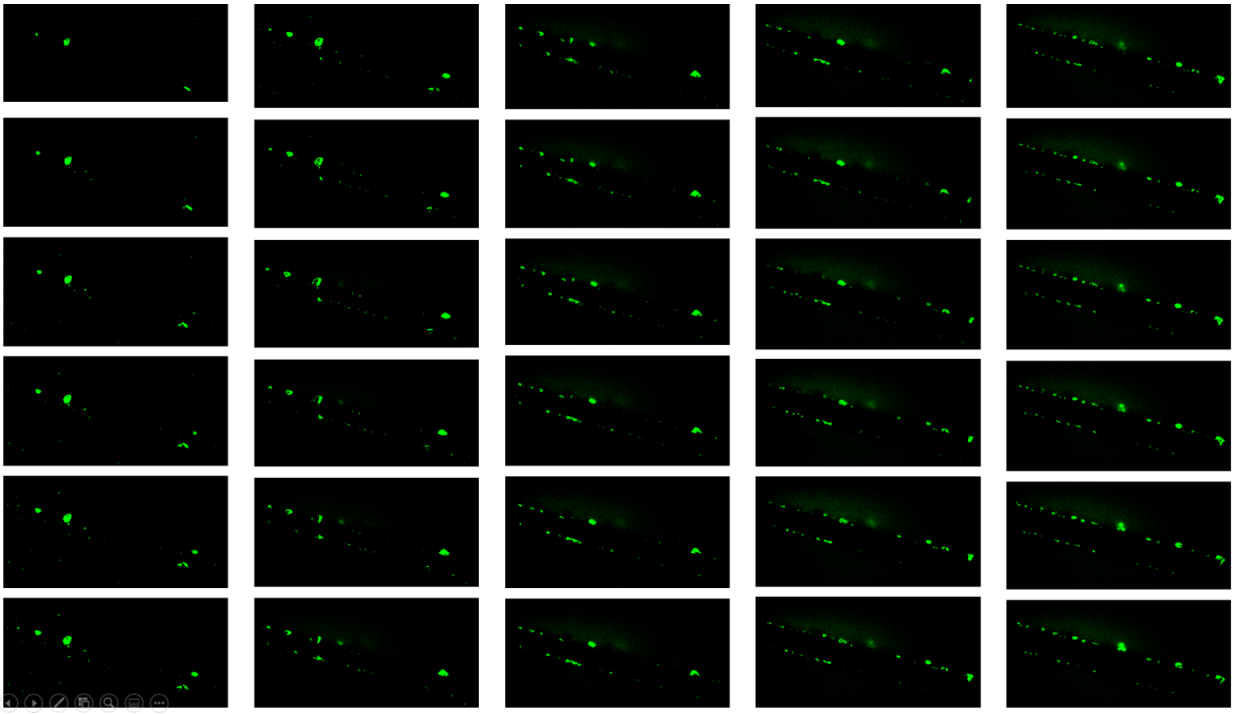

Figure S21: Selected confocal image sequence of Figure 2. Each image is a 100 nm step in the z direction (bottom towards top). Sequence order: ↓↗↓↗↓↗↓↗↓.

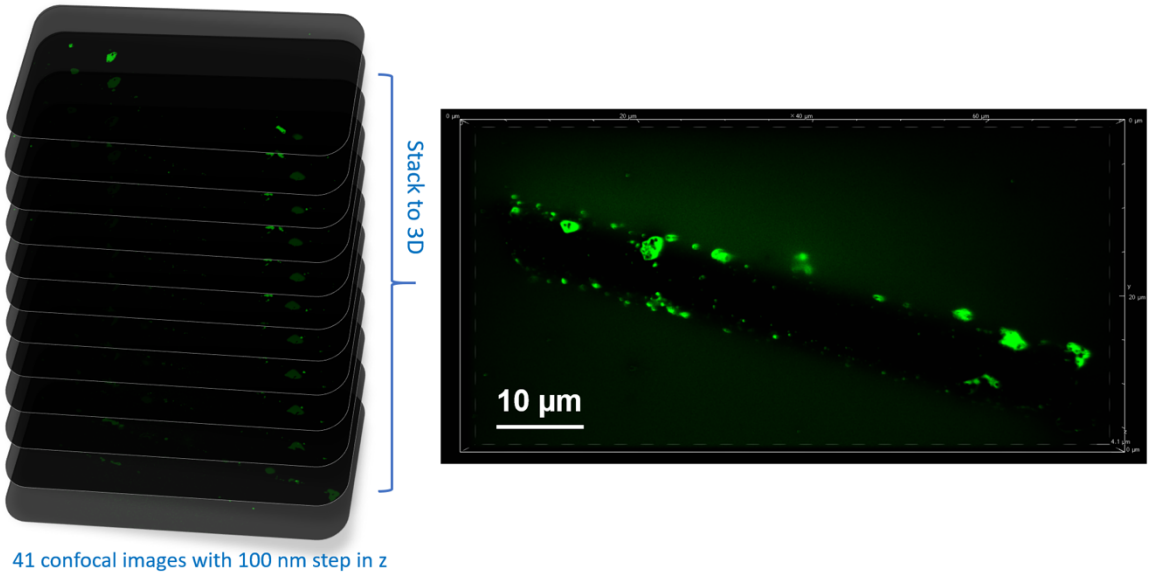

Figure S22: 3D image by 41 2D confocal image stack in z. The z step is 100 nm. Note: A video showing these data as the confocal plane gradually travels along the z plane is also available as supporting information.

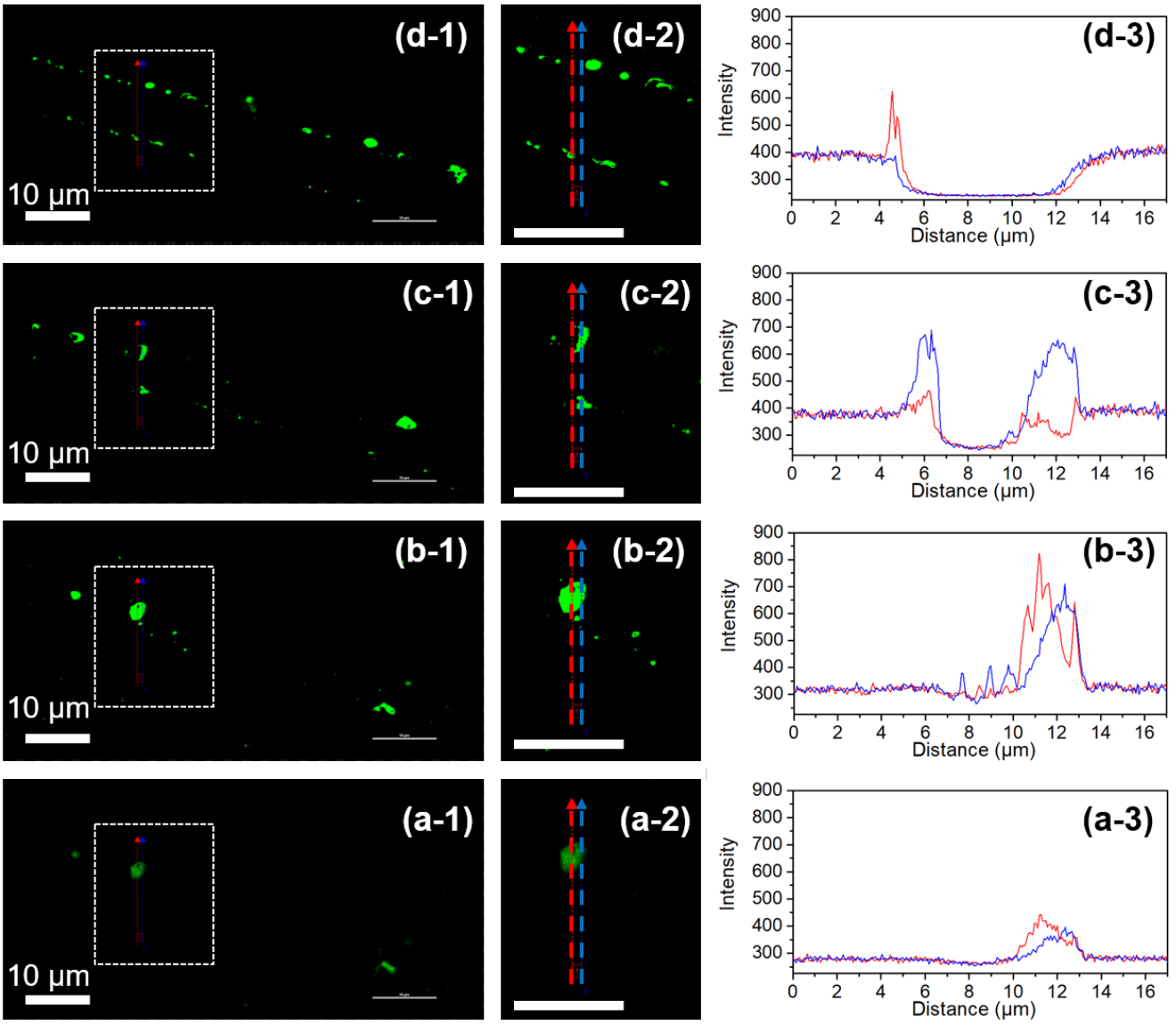

Figure S23: Confocal intensity profile across a Pd@GW catalyst at different z-step. The corresponding confocal images a-d were shown at Figure 2 (a-d).

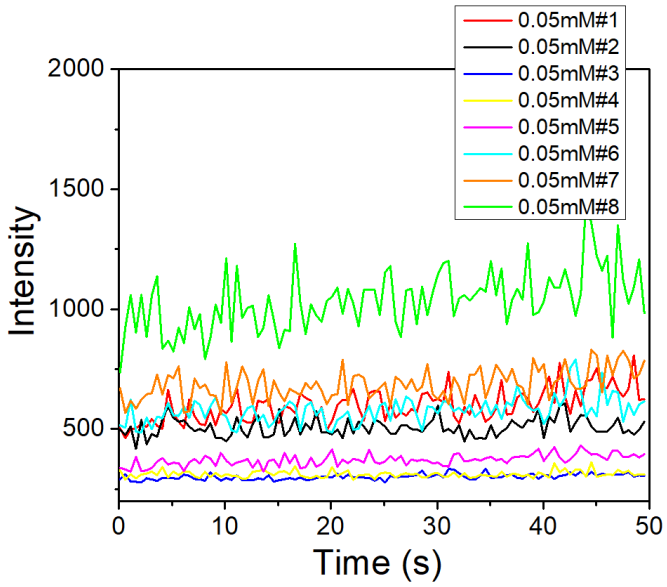

Figure S24: Confocal fluorescence intensity traces of selected areas of 0.05 mM NN1 reaction. The area positions are shown in Figure 7 in the main manuscript. The spots number and position are shown in Figure 4 of the manuscript.

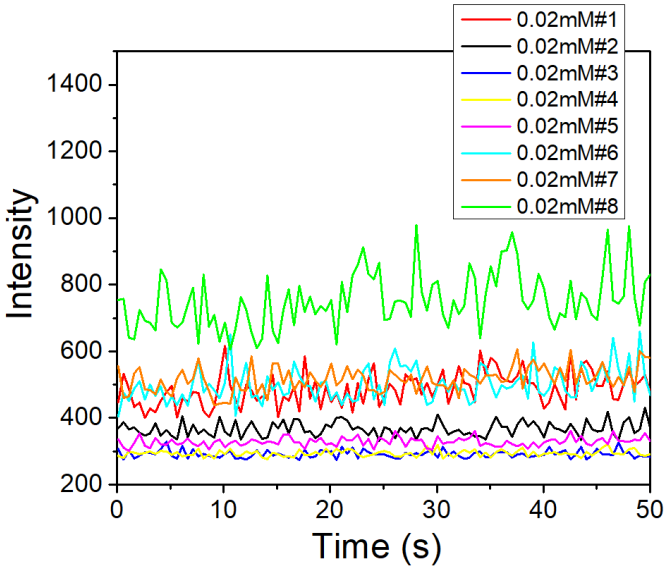

a

Figure S25: Confocal fluorescence intensity traces of selected areas of 0.02 mM NN1 reaction. The area positions are shown in Figure 7 in the main manuscript. The spots number and position are shown in Figure 4 of the manuscript.

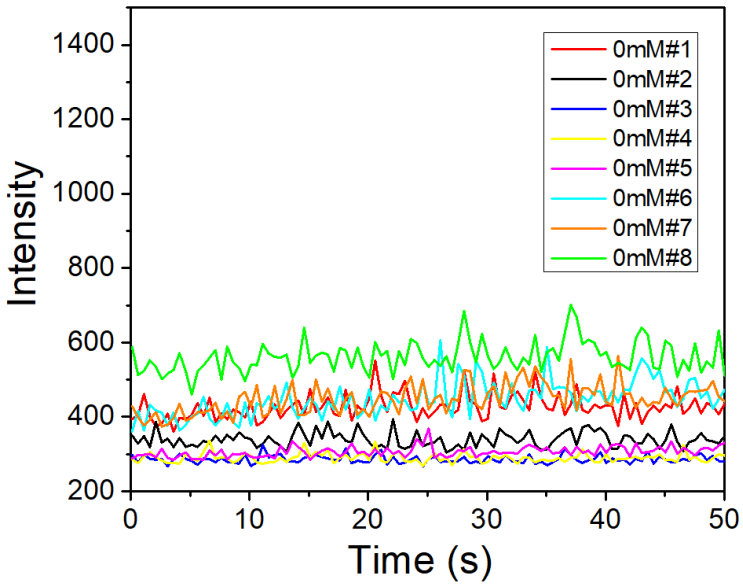

Figure S26: Confocal fluorescence intensity traces of selected areas after H_2O washing (0.3 mL). The area positions are shown in Figure 7 of the main manuscript. The spots number and position are shown in Figure 4 of the manuscript.

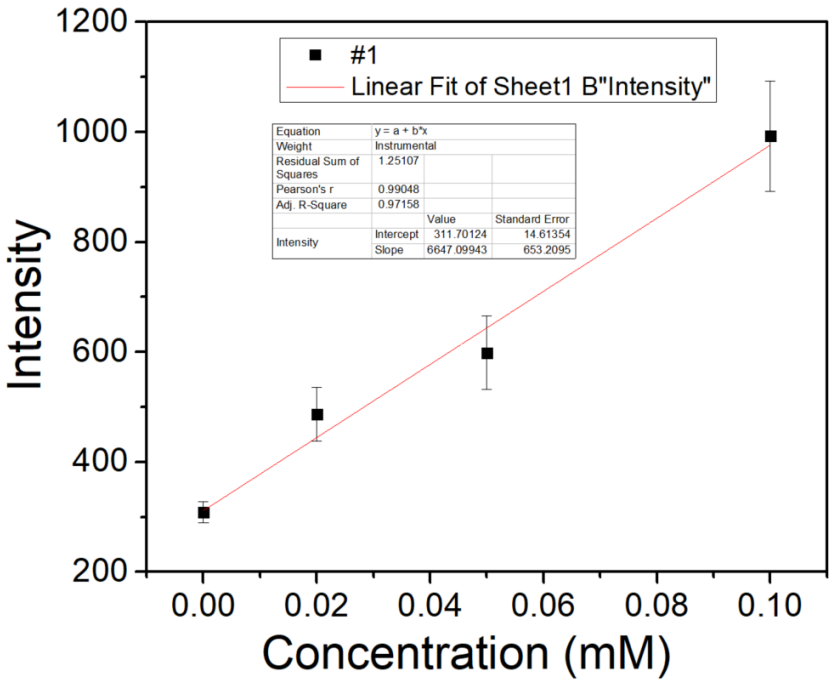

Figure S27: Fluorescence intensity as a function of reaction concentration of position #1. The area positions are shown in Figure 7 of the main manuscript. The spots number and position are shown in Figure 4 of the manuscript.

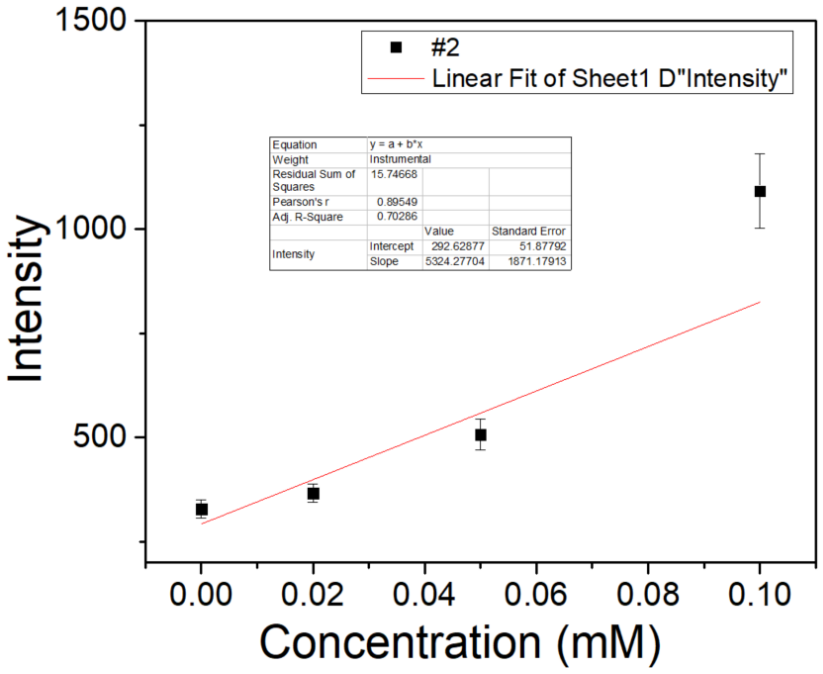

Figure S28: Fluorescence intensity as a function of reaction concentration of position #2. The area positions are shown in Figure 7 of the main manuscript. The spots number and position are shown in Figure 4 of the manuscript.

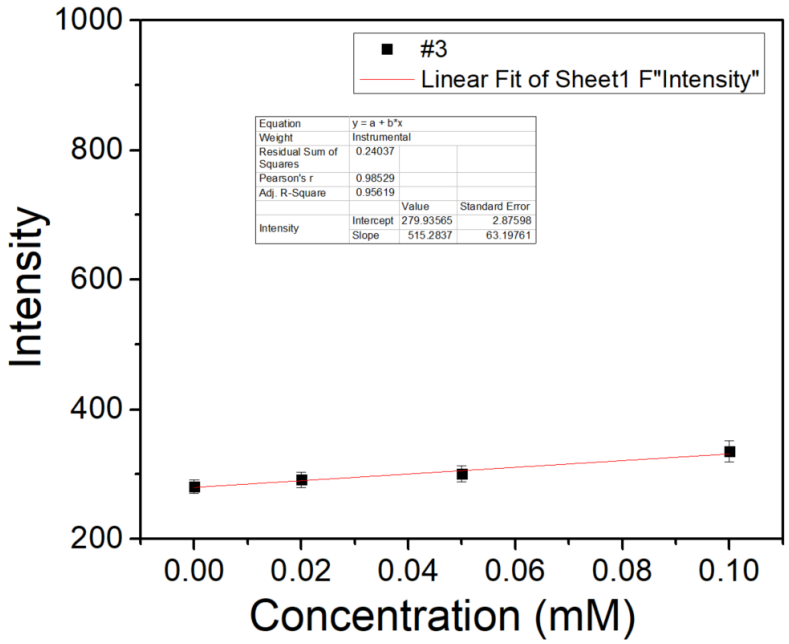

Figure S29: Fluorescence intensity as a function of reaction concentration of position #3. #3 is the inert representative area of Pd@GW without Pd particles. The area positions are shown in Figure 7 of the main manuscript. The spots number and position are shown in Figure 4 of the manuscript.

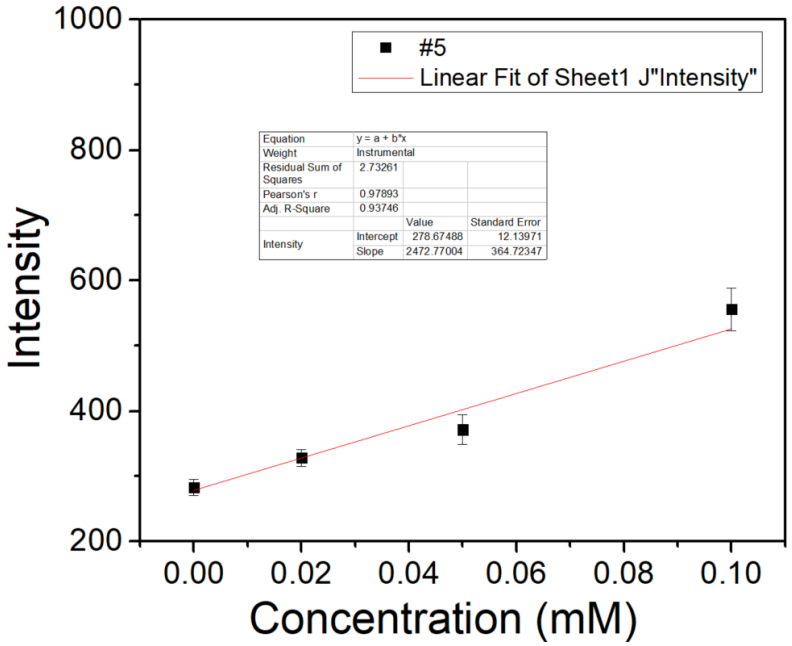

Figure S30: Fluorescence intensity as a function of reaction concentration of position #5 (representative background). The area positions are shown in Figure 7 of the main manuscript. The spots number and position are shown in Figure 4 of the manuscript.

~~8~~7 Single-molecule Microscopy data

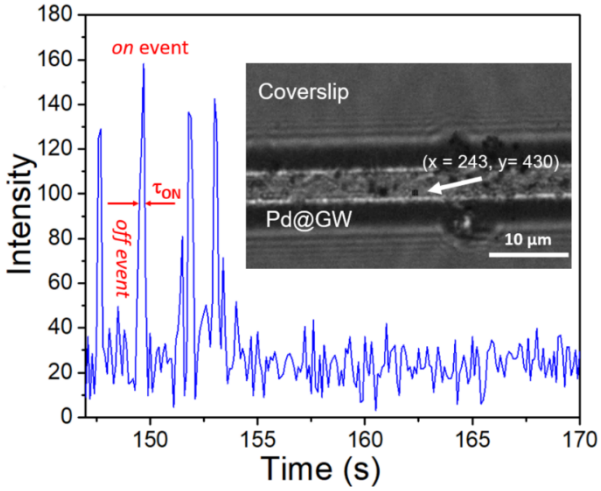

Figure S31: Segment of a typical emission trajectory of one catalytic area on Pd@GW. Data points captured every 100 ms. Inset: white light images of the selected area for 1µM NN1 reacting with 160µL of 0.035% N_2H_4 in the presence of 100 µL of 33 mM acetic acid. The white light of Pd@GW is shown in Figure S32. A top view of 3D confocal image of same fiber was shown in Figure S33.

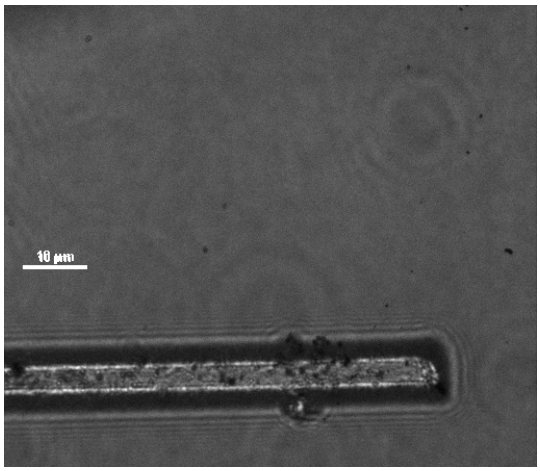

Figure S32: White light image of Pd@GW, the scale bar is 10 µm.

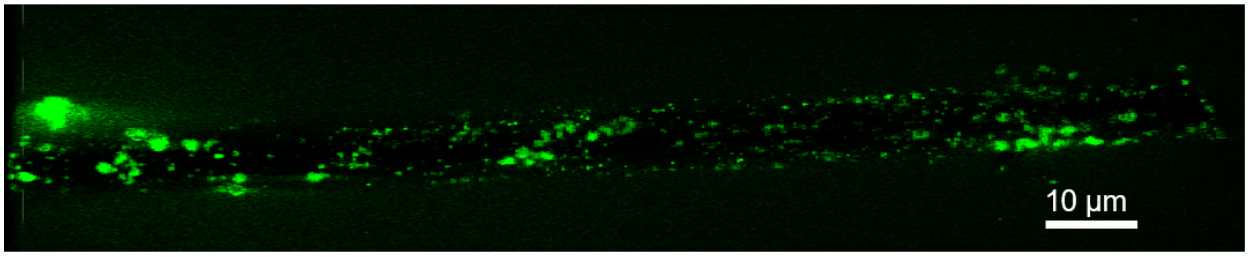

Figure S33: Confocal fluorescence image (2D sum of 9 z-planes) of a ~130 μm long fiber decorated with Pd. Each z-step is 500nm. The white light image if this fiber was shown in Figure S 32.

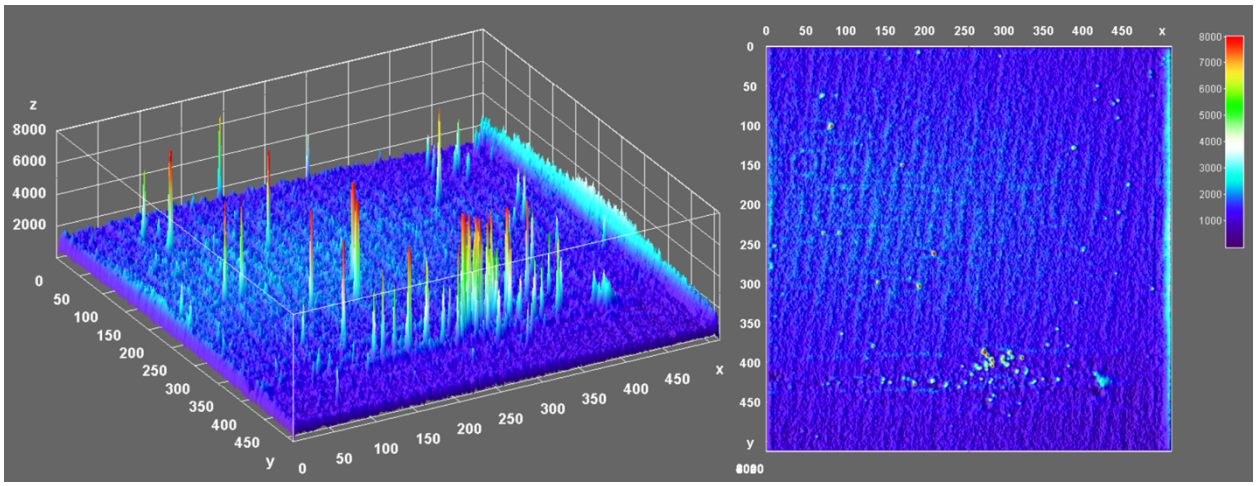

Figure S34: 3D image and intensity stack images of 3000 frames. In the right image the Pd@GW fiber segment used is located approximately at 430 in the y-scale. Each pixel is ~160 nm.

Based on the same acquisition as in Figure S34, the data were separated in the first and second sets of 1500 images each (or 150 s). Comparison of the images in Figures S35 and S36 below shows many similarities, but they are not identical. Particularly the region in the vicinity of y~400 and x~300 shows minor, but detectable changes, suggesting that some sites change in their catalytic activity for two sequential 150 second periods, or some mobility of Pd catalytic sites. Overall these changes are quite minor.

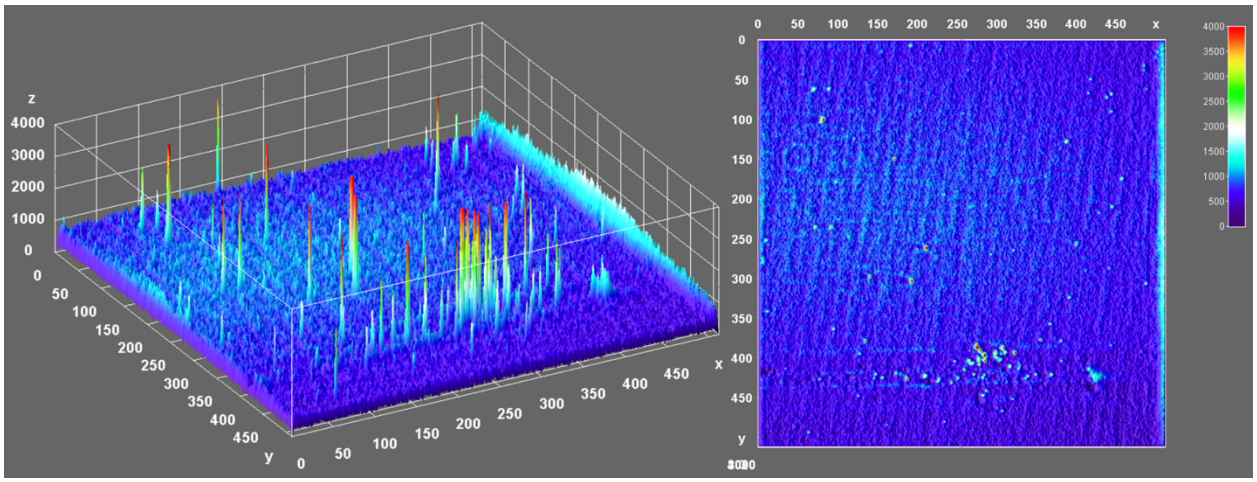

Figure S35: 3D image and intensity stack images of 1-1500 frames (150 seconds).

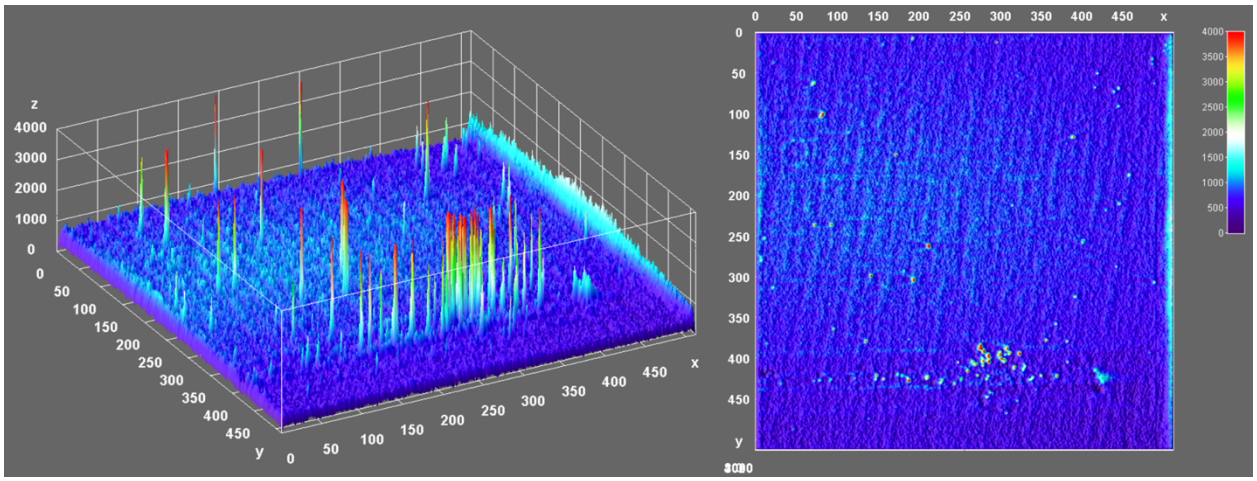

Figure S36: 3D image and intensity stack images of 1501-3000 frames (150 seconds).

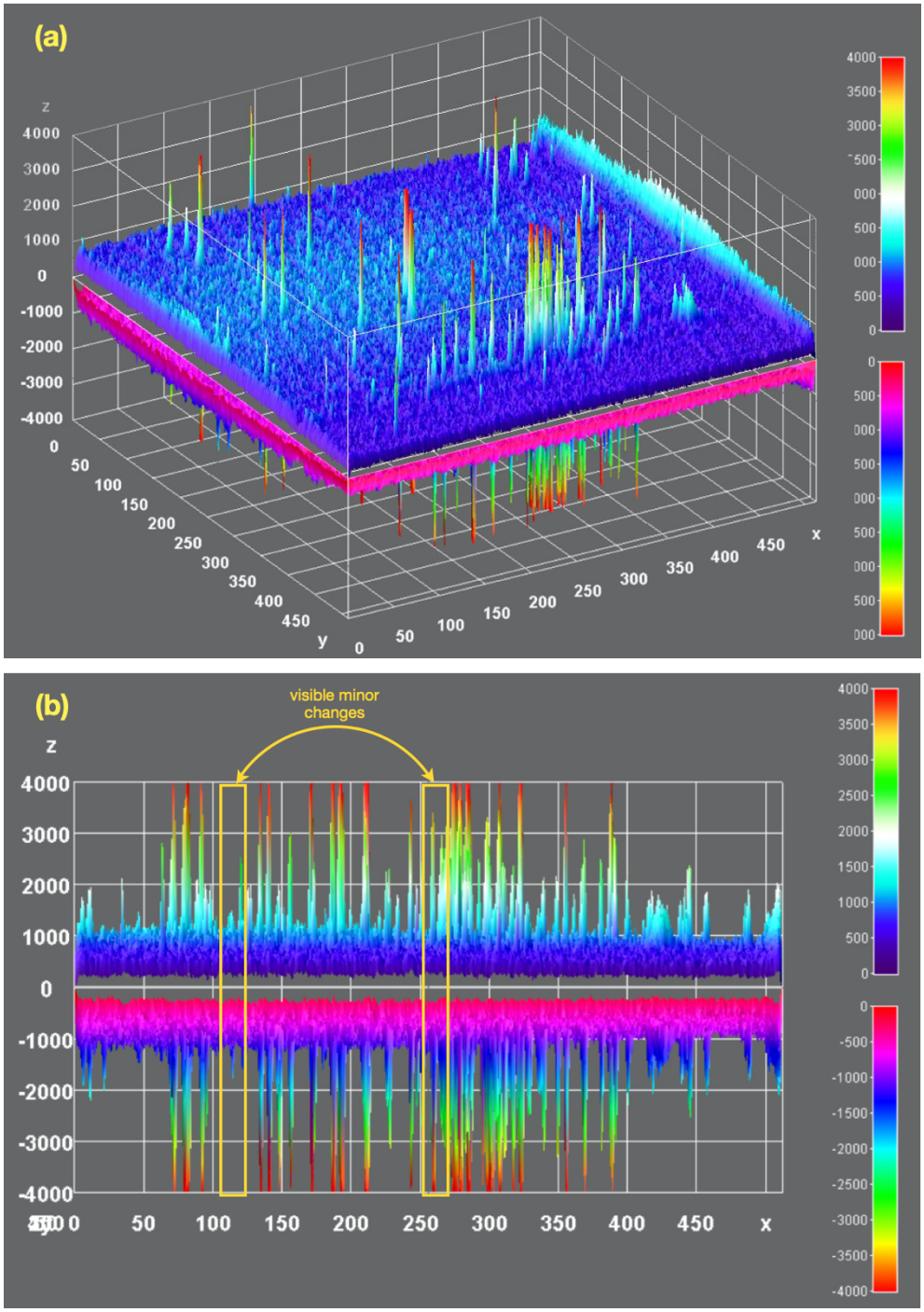

Figure S37: Images of the first 1500 frames (top) and second 1500 frames (inverted, shown at bottom); (a) 3D plot; (b) view from the edge of the x-y plane. Note that the vast majority of the plot features do not change. Detailed observation in the yellow rectangle enclosures do undergo minor changes in site activity when two 150 s acquisitions are compared.

~~9~~8 Optical and Electron Microscopy Images

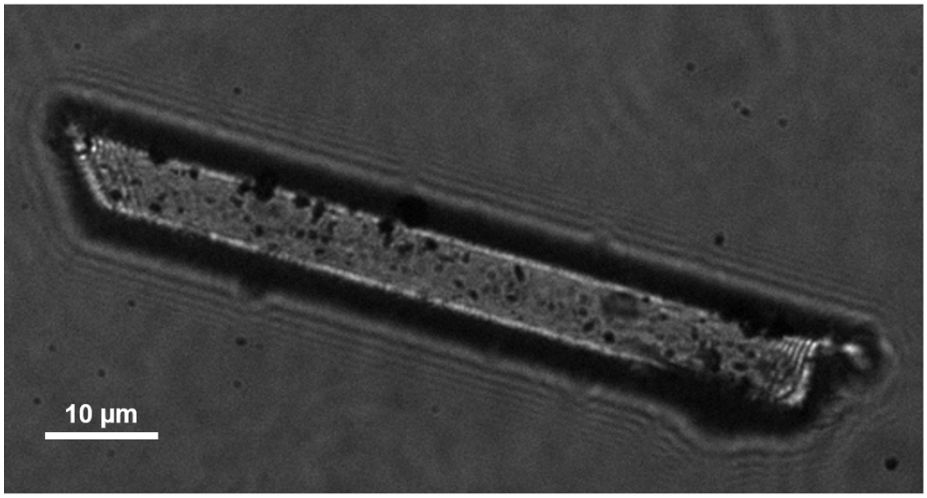

Figure S38: White light image of Pd@GW in Figure 4. Scale bar is 10 µm. The optical image is mirror image of confocal image.

~~10~~9 SEM and Confocal co-localized analysis

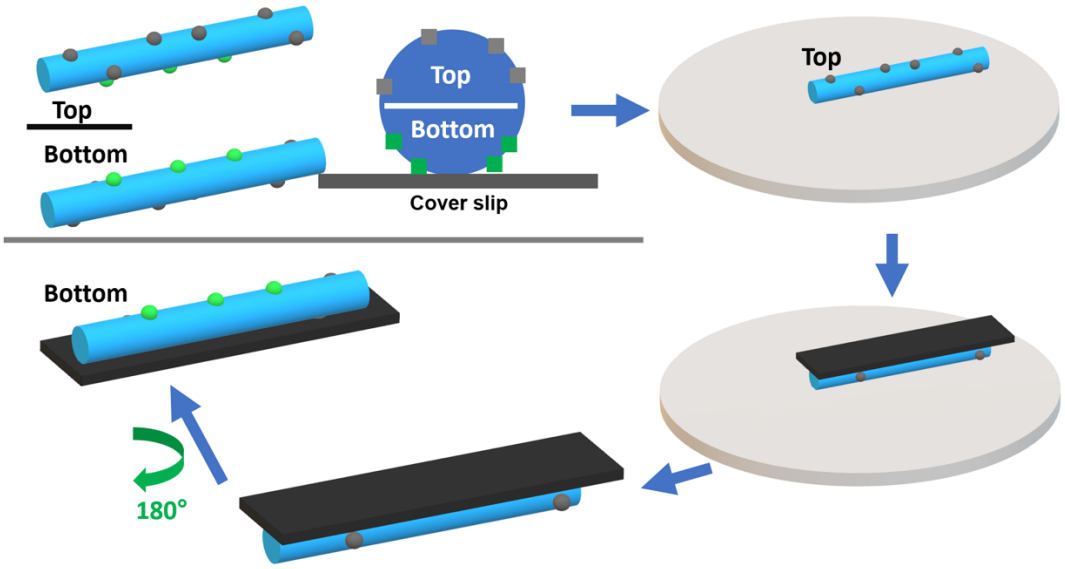

Figure S39: Inversion process of Pd@GW catalyst on cover slip. In this process carbon tape is used to flip the glass fiber, revealing the bottom region of the fiber- the same region which is imaged using confocal microscopy.

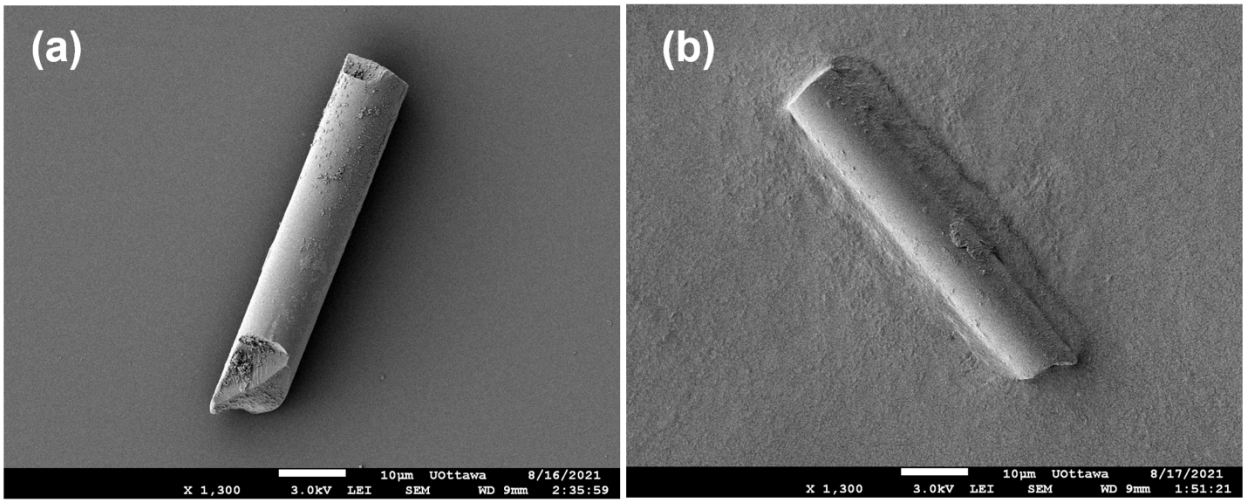

Figure S40: Original SEM image of figure 5, (a) SEM top view, (b) SEM bottom view of same Pd@GW fiber after inversion by SEM conductive tape.

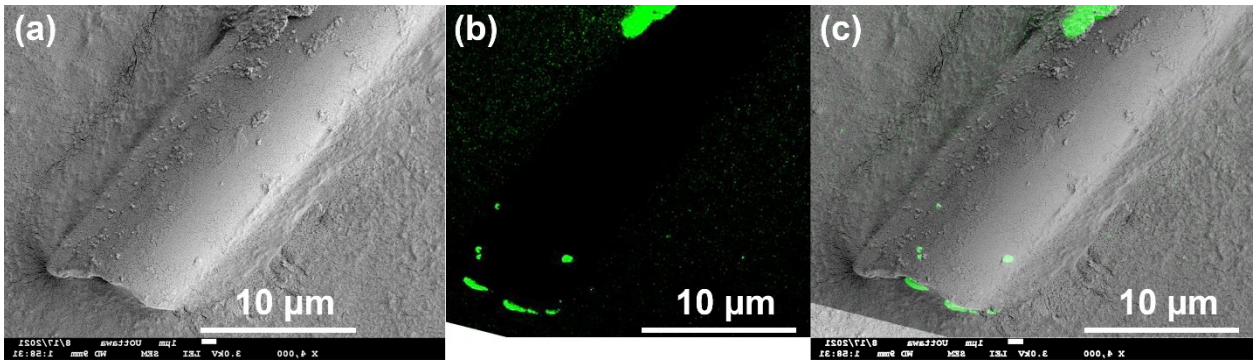

Figure S41: Magnified SEM (a) and confocal (b) images of Pd@GW, and superimposed confocal/SEM combined image (c).

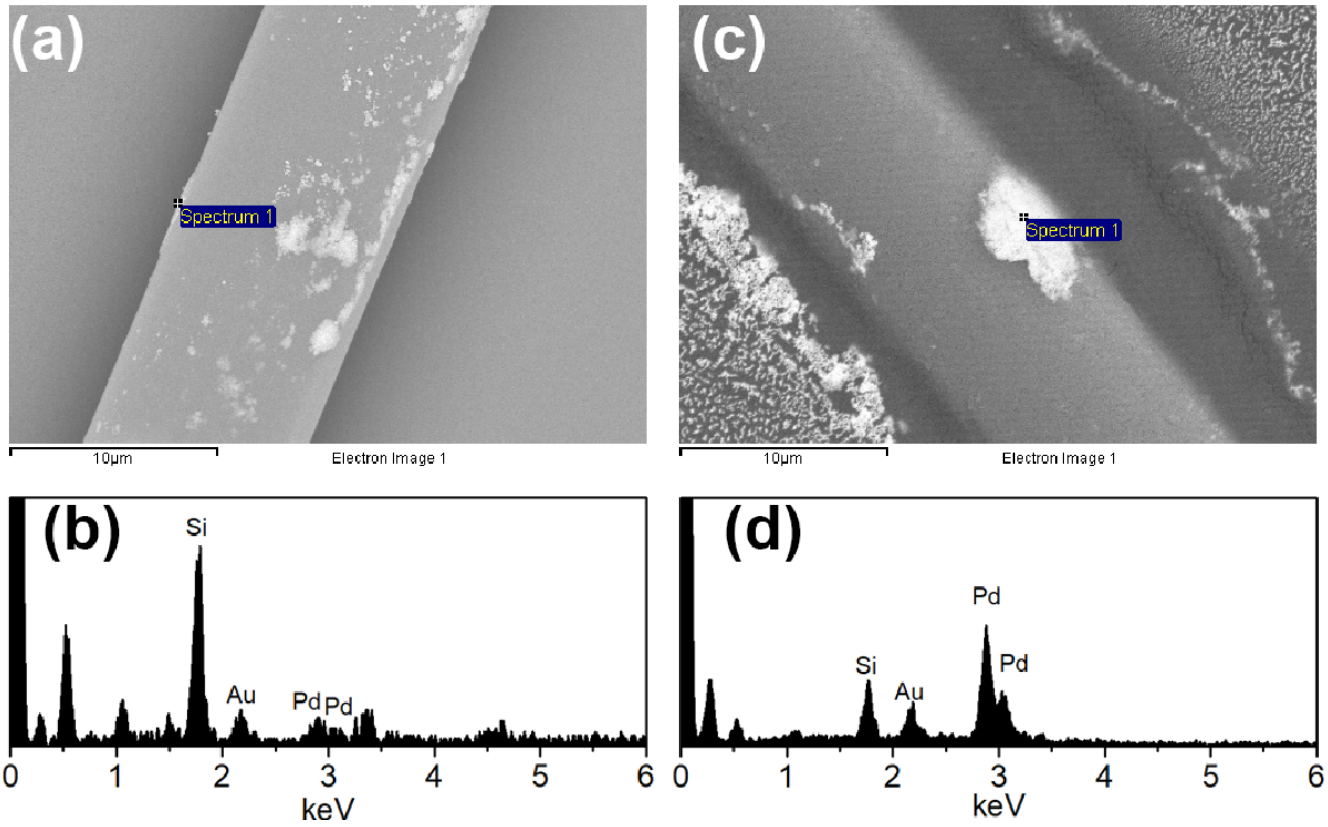

Figure S42: SEM images and corresponding EDS analysis of Pd@GW before (a-b) and after inversion c-d).

~~11~~10 FLIM data

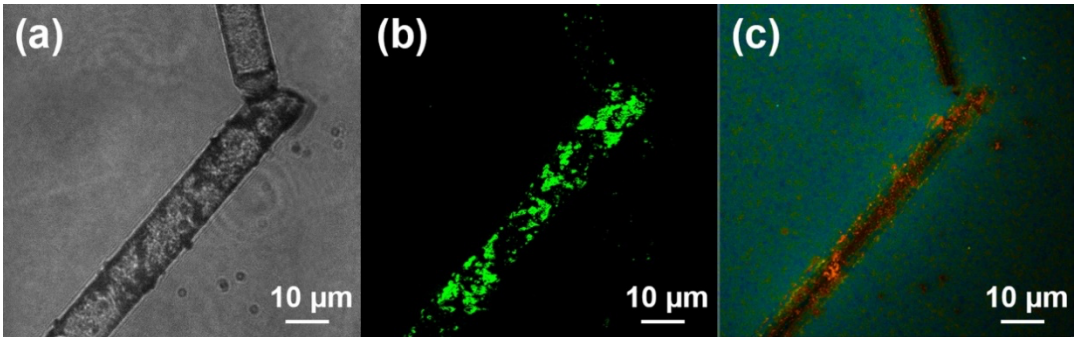

Figure S43: White light transmission (a), confocal 3D stack image (b) and FLIM image (c) of the same fibers.

The FLIM intensity and lifetime profile analysis are shown in Figure S44. The lifetime and intensity traces of surface region of Pd@GW are shown in (a, b). The lifetime dropped to 1.7 ns and the intensity increases to ~60 when the products are close to the Pd particles. Due to the cylinder structure of glass wool, the detectors are not able to receive photons from the inside of the catalyst. The photon intensity is almost zero from 9.5 to 18.0 µm at x-axis and 8.5 to 19.5 µm at y-axis as shown in Figure S44 (f). The lifetime traces of internal structure (~10-18 µm) were not accurate because of the low photon number. It is worth pointing out that the intensity jumps to ~60 when the profile line crosses the Pd structure (see arrows in (f) and (g)), and its lifetime decrease to around 2 ns closed to Pd particles.

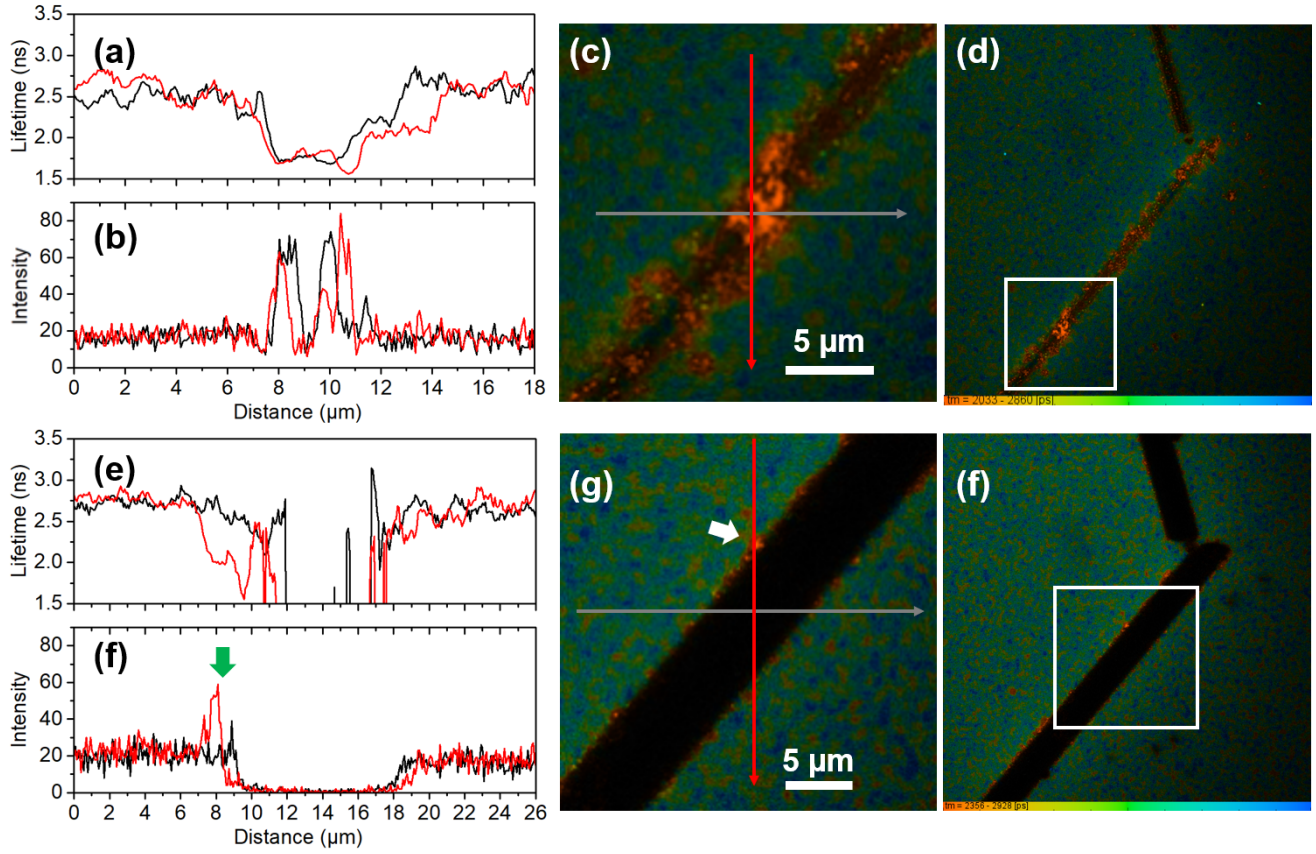

Figure S44: Lifetime profile (a, e) and FLIM intensity profile (b, f) across a Pd@GW catalyst at different z-step (a-d: 0.2 μm; e-f: 1.4 μm). The cross-profile lines were shown in (c) and (g), the original FLIM figures were shown in (d) and (f), the white square was the selected ROI.

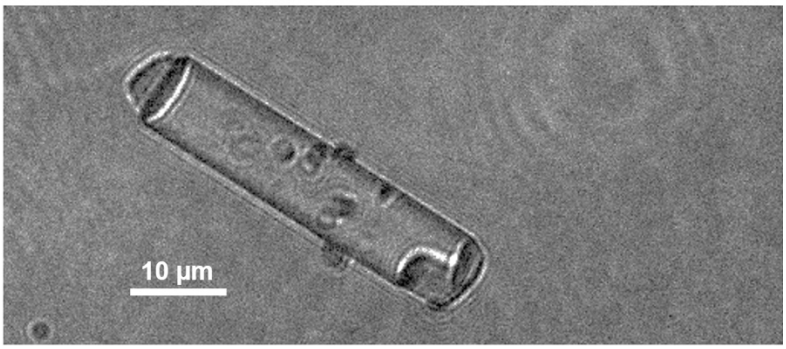

Figure S45: White light image of catalytic fiber in Figure 8.

Table S1: Confocal z-stack step depth analysis of Figure 6.

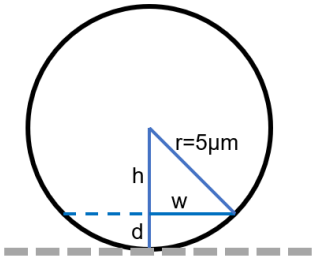

$$d = r - \sqrt{r^2 - w^2}$$

Where:
r: Pd@GW radius ~ 5 µm
w: half width of cross profile from FLIM and confocal images
d: distance of cross profile from coverslip

	Width (µm)	Height (µm)	d (µm)
a, b	8.05	2.97	2.03
c, d	6.9	3.62	1.38
e, f	5.25	4.26	0.74
g, h	2.83	4.80	0.20
I, j	2.05	4.89	0.11

~~12~~11 References

1. Wang, B.; Lanterna, A. E.; Scaiano, J. C., Mechanistic Insights on the Semihydrogenation of Alkynes over Different Nanostructured Photocatalysts. *ACS Catalysis* **2021,** *11* (7), 4230-4238.
2. Elhage, A.; Wang, B.; Marina, N.; Marin, M. L.; Cruz, M.; Lanterna, A. E.; Scaiano, J. C., Glass wool: a novel support for heterogeneous catalysis. *Chem Sci* **2018,** *9* (33), 6844-6852.
3. Scaiano, J. C.; Stamplecoskie, K. G.; Hallett-Tapley, G. L., Photochemical Norrish type I reaction as a tool for metal nanoparticle synthesis: importance of proton coupled electron transfer. *Chem Commun (Camb)* **2012,** *48* (40), 4798-808.
4. Corma, A.; Concepcion, P.; Serna, P., A different reaction pathway for the reduction of aromatic nitro compounds on gold catalysts. *Angewandte Chemie* **2007,** *46* (38), 7266-9.
5. Dai, Y.; Li, C.; Shen, Y.; Lim, T.; Xu, J.; Li, Y.; Niemantsverdriet, H.; Besenbacher, F.; Lock, N.; Su, R., Light-tuned selective photosynthesis of azo- and azoxy-aromatics using graphitic C3N4. *Nat Commun* **2018,** *9* (1), 60.